Contrib Mineral Petrol (2003) 145: 424–443
DOI 10.1007/s00410-003-0465-y

ORIGINAL PAPER

**Lawrence A. Taylor · Gregory A. Snyder
Randall Keller · David A. Remley · Mahesh Anand
Rene Wiesli · John Valley · Nikolai V. Sobolev**

Petrogenesis of group A eclogites and websterites: evidence from the Obnazhennaya kimberlite, Yakutia

Received: 21 April 2002 / Accepted: 14 February 2003 / Published online: 7 May 2003

Abstract Mantle xenoliths from the Obnazhennaya kimberlite pipe, Yakutia, possess a large range of mineralogical and chemical compositions, from both group A and B eclogites. Major-element contents of the group A eclogites exhibit transitional features between the group B eclogites and peridotite. The Mg# of clinopyroxenes is 0.86–0.94, with 0.60–0.84 for garnets. Differences in concentration of LREEs exist between the Obnazhennaya group A and the well-studied group B eclogites from the Udachnaya kimberlite pipe. In general, garnets in the group A eclogites contain lower LREEs than those from the group B eclogites; however, the trend for clinopyroxene is reversed. High $\delta^{18}O$ (5.46–7.81) values, and the positive Eu anomalies in the garnets and clinopyroxenes (Eu/Eu* 1.2–1.4) demonstrate the involvement of an oceanic crustal component in the formation of the group A eclogites. The group A eclogites formed between 21.0 and 37.6 kbar, and 711 and 923 °C, in a time interval of 1,071–1,237 Ma. An innovative model is proposed to explain the formation of the group A eclogites and websterites. It involves the reaction of a depleted mantle peridotite with TTG and carbonatite melts closely related to the subduction of oceanic crust.

L. A. Taylor (✉) · G. A. Snyder · R. Keller · D. A. Remley
M. Anand · R. Wiesli
Planetary Geosciences Institute, Department of Earth Planetary Sciences, University of Tennessee, Knoxville, TN, 37996-1410, USA
E-mail: lataylor@utk.edu
Tel.: +1-865-9746013
Fax: +1-865-9746022

J. Valley
Department of Geology and Geophysics,
University of Wisconsin, Madison, WI, 53706, USA

N. V. Sobolev
Institute of Mineralogy and Petrography,
Russian Academy of Science, Novosibirsk, Russia

Editorial responsibility: T. Grove

Introduction

The mantle comprises 80% by volume of the Earth and is the progenitor of the crust. However, we still have much to learn about the chemical composition and petrogenesis of the mantle, which is requisite to understanding the complex evolution of the Earth. Deep-seated xenoliths, in a variety of lithologies, found in alkali basalts and kimberlites around the world, provide samplings of material from the uppermost portion of the mantle; the majority of such xenoliths come from the continental lithosphere. These xenoliths include dunites, lherzolites, harzburgites, wehrlites, eclogites, pyroxenites, and websterites. Garnet-, spinel-, and diamond-bearing varieties of these rocks are also known. In total, these samples present snapshots of the geochemical processes which occur deep within the Earth.

Mantle eclogites, one of the two major types of diamondiferous xenoliths, are composed mainly of garnet and clinopyroxene. Bulk compositions of these eclogites may range from olivine basalt to tholeiitic basalt and anorthositic gabbro (e.g., Coleman et al. 1965; Shervais et al. 1988). Taylor and Neal (1989) subdivided this range of mantle eclogite compositions into three groups (A, B, and C), according to the chemical scheme of Coleman et al. (1965). Group B and C eclogites are generally bimineralic, composed of garnets rich in almandine, as well as grossular components, and omphacitic clinopyroxenes, with intermediate- to high-jadeite components. Group C also entails rare occurrences of grospydites, i.e., kyanite and corundum eclogites. It has been widely accepted that group B and C eclogites represent relicts of different stratigraphic levels of ancient oceanic crust which were metamorphosed during subduction into the mantle (e.g., Helmstaedt and Doig 1975; MacGregor and Manton 1986; Shervais et al. 1988; Taylor and Neal 1989; Neal et al. 1990; Jerde et al. 1993; Ireland et al. 1994; Snyder et al. 1995; Beard et al. 1996; Snyder et al. 1997).

In contrast to group B and C eclogites, the group A eclogites contain pyropic garnets, relatively rich in Cr_2O_3 (0.3 to 0.6 wt%), and have been considered to be of true mantle origin (e.g., Taylor and Neal 1989; Snyder et al. 1997). Clinopyroxenes from this group also have high ratios of Mg/(Mg + Fe), low-jadeite components, and relatively high Cr_2O_3 contents (0.2 up to 1.5 wt%). Orthopyroxene and/or olivine may also occur as minor (< 1%) accessory minerals. When these rocks contain primary orthopyroxene, they are not eclogites *sensu stricto* but are properly referred to as garnet websterites. Because of the relatively small size of the xenoliths in the present study (< 50–75 g), it is not always realistic to give different petrologic names to these rocks based upon a few thin sections. In this study, any xenolith with orthopyroxene, in addition to garnet and clinopyroxene, has been designated as garnet websterite. However, because of the distinct similarities in mineral compositions of group A eclogites with websterites, their petrogeneses have been treated together.

Compared with those of group B and C, previous studies of group A eclogites have indicated virtually no evidence of oceanic crustal affinity. However, petrogenetic models of group A eclogites are controversial, and their origin remains an enigma. Some workers have concluded that these xenoliths are samples from direct igneous activity in the mantle (e.g., Shervais et al. 1988; Smyth et al. 1989; Neal et al. 1990; Snyder et al. 1995, 1997). Others have speculated that these samples may be of oceanic affinity, being remnants of deeper, ultramafic oceanic crust, akin to the harzburgitic to gabbroic sections of ophiolites (e.g., MacGregor and Manton 1986; Jacob et al. 1994; also see Snyder et al. 1997, 1998, for a discussion). It is also believed that in the Archean, the ocean-ridge basalts were relatively more mafic, and these may have been involved in the genesis of some of the group A eclogites of Archean ages. It is to the origin of group A eclogites that this paper is directed, utilizing a unique suite of eclogites and garnet websterites from a well-known, albeit non-diamondiferous Siberian kimberlite.

The Obnazhennaya kimberlite is one of the many pipes in Yakutia (Fig. 1) and, unlike many other Siberian locales, this kimberlite is non-diamondiferous and provides information on a relatively shallower region (i.e., within the graphite stability field) of the subcratonic Siberian mantle near the northeast edge of the platform (Sobolev 1977; Ouchinnikov 1989; Spetsius and Serenko 1990). A large number of xenoliths from this pipe are of group A eclogites and websterites (Qi et al. 1994, 1997). In this report, a suite of eclogites and websterite xenoliths, in addition to some peridotites from the Obnazhennaya kimberlite pipe, have been selected for detailed mineralogical, petrological, and geochemical studies, with emphasis on addressing the origin of the group A eclogites and websterites.

Geological setting

The Siberian platform comprises a large expanse of north-central Asia (Fig. 1). The platform extends more than 2,500 km from Lake Baikal in the south, northwards to the Arctic Ocean, and from the Sea of Okhotsk in the east to the Yenisey River in the west. Geophysical studies suggest that the Moho occurs at depths of 35–60 km beneath the platform (Rosen et al. 1994). The platform consists of a variety of Precambrian rocks

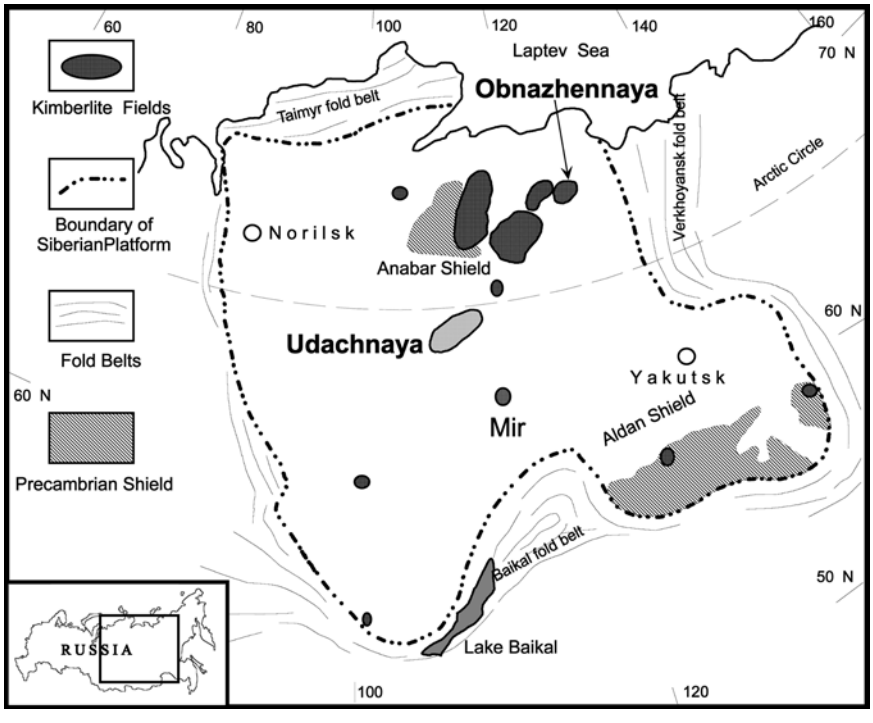

Fig. 1 Simplified geological map of the Siberian platform indicating kimberlite fields, fold belts, and surface expressions of Precambrian rocks. The Obnazhennaya kimberlite pipe, from which the studied xenoliths come, is located at the northeastern margin of the platform

overlain by Phanerozoic sedimentary sequences. Major suture zones, which are Phanerozoic in age, bound the platform and formed during the accretion of Pangea (Zonenshain et al. 1990). The basement rocks of the platform have been subdivided into seven crustal provinces, according to when they were accreted onto the craton (Rosen et al. 1994). Three provinces, Olenek, Anabar, and Magan, are known to contain kimberlite intrusions. These intraplate magmatisms occurred during the Paleozoic and Mesozoic eras (Sobolev 1977; Zonenshain et al. 1990).

The Obnazhennaya kimberlite pipe is located within the lower Olenek province which occupies the extreme northeastern portion of the platform (Fig. 1), along the lower portion of the Olenek River, near the Kuoika River. The pipe is exposed in a riverbank-cliff outcrop, and it is a small intrusion with an elliptical shape of approximately 30 by 45 m. A large amount of kimberlitic breccia occurs at this locality, composed of kimberlite matrix with a plethora of olivine fragments and a variety of mantle xenoliths (Sobolev 1977). The Obnazhennaya kimberlite intruded Sinian dolomites during the late Jurassic, which is confirmed both by the finding of a fossil belemnite in the kimberlite (Milashev and Shul'gina 1959) and by U–Pb dating of zircons (Davis et al. 1980).

The Obnazhennaya xenolith suite

The Obnazhennaya kimberlite displays a range of xenolith compositions from ultramafic to mafic. Unique amongst the Yakutian kimberlites, there is a continuous gradation in xenolith composition, from peridotite to eclogite. The mineral associations recorded in the rocks include (1) garnet + olivine + orthopyroxene + clinopyroxene (peridotite); (2) garnet + clinopyroxene + orthopyroxene (websterite); (3) garnet + clinopyroxene (eclogite, groups A and B); and (4) olivine (dunite). All xenoliths and the kimberlite are barren of diamond. Secondary features which occur in these rocks include phases formed by metasomatic reaction, both at depth, and with the host kimberlite. Exsolutions of garnet, corundum, and orthopyroxene are common in clinopyroxene, and rutile exsolution occurs in many garnets.

Peridotite is the most abundant xenolith in Obnazhennaya, including garnet-lherzolite and spinel-lherzolite (Sobolev 1977; Spetsius and Serenko 1990). These xenoliths are composed of forsterite-rich olivine (Fo 90–92), Cr-diopside, orthopyroxene, garnet and/or spinel, and commonly contain a sulfide assemblage of chalcopyrite + pyrrhotite + pentlandite. Although these rocks are all ultramafic in composition, they possess wide chemical variations which are reflected in the modes and mineralogy of the rocks. With decreasing amounts of olivine, there is an overall increase in the proportion of pyroxene and garnet (Sobolev 1977), thereby extending from ultramafic to mafic compositions. Significant variations also are found in the Cr_2O_3 contents of these xenoliths.

Eclogite is the second most abundant xenolith in the Obnazhennaya kimberlite, and also shows significant variations in mineralogy and chemical composition. Websterites are the third most abundant. Eclogites are divided into different groups, among which the abundance of group A eclogites is greater than that of group B. Unusual corundum-bearing eclogite xenoliths (e.g., O-160; Sobolev 1977; Qi et al. 1997) are also reported from the Obnazhennaya kimberlite, but they are rare. This type of rock, under-saturated in silica, differs from the other eclogites in its high CaO and Al_2O_3 contents (Sobolev 1977; Spetsius and Serenko 1990), manifested as abundant ruby, in addition to large clinopyroxenes (2–5 cm) which display a varied array of exsolutions, i.e., orthopyroxene, garnet, corundum, kyanite, and sanadine (Qi et al. 1994, 1997).

Petrography

The mineralogy and textures of the Obnazhennaya xenoliths are relatively simple, due largely to their generally unweathered nature, lack of secondary minerals, and absence of primary hydrous phases. From our large collection, 25 xenoliths were selected for detailed study, including seven peridotitic, eight eclogitic, and ten websteritic xenoliths (Table 1). The modal compositions of the non-peridotite xenoliths are also listed in Table 1. It should be noted that large uncertainties ($\pm 10\%$) are associated with the modal estimates, due to the coarse-grained nature (1–3 cm) and small sizes of the samples (0.05–1 kg).

Garnet-websterite xenoliths

Ten samples (O-4, O-81/91, O-83/91, O-84/91, O-85/91, O-86/91, O-901, O-1085, O-1101, O-1109) have textures similar to cumulate rocks and consist of bright green, coarse-grained clinopyroxene crystals which range in size from 12.5 to 30 mm. Pale pink, coarse-grained anhedral garnets with irregular geometry occur as interstitial material between these large clinopyroxenes. Garnets range in size from 3 to 6 mm, and display moderate rutile exsolution along {111} crystallographic planes. Orthopyroxene (2–12.5 modal%), 1.5 to 3.0 mm in size, occurs as anhedral grains between garnet crystals. Some orthopyroxenes contain significant ilmenite lamellae, likely formed as secondary exsolution.

Eclogite xenoliths

Samples O-82/91, O-423, O-501, O-926, O-927, O-1073, O-1103, and O-1108 consist of coarsely interlocking mosaics of subhedral garnet and clinopyroxene. These xenoliths are composed of dark green clinopyroxene and pale orange–pink garnets. Clinopyroxene crystals range in size from 5 to 25 mm, with garnets from 1.5 to

Table 1 Xenoliths studied from the Obnazhennaya kimberlite pipe, with modal analyses for eclogites and websterites

Sample	Rock (group)	Garnet	Clinopyroxene	Orthopyroxene	Spinel
O-82/91	Eclogite (B)	70.8	27.7		1.5
O-423	Eclogite (A)	26.8	73.2		
O-501	Eclogite (B)	54.1	45.9		
O-926	Eclogite (A)	31.5	68.5		
O-927	Eclogite (B)	32.3	67.7		
O-1073	Eclogite (A)	36.3	63.7		
O-1103	Eclogite (A)	42.1	57.9		
O-1108	Eclogite (A)	31.2	68.8		
O-4	Websterite (A)	32.7	63.4	3.9	
O-81/91	Websterite (A)	55.9	32.3	11.8	
O-83/91	Websterite (A)	48.3	46.5	5.2	
O-84/91	Websterite (A)	39.4	47.9	12.5	0.2
O-85/91	Websterite (A)	45.3	52.8	1.5	0.4
O-86/91	Websterite (A)	39.8	51.2	8.7	0.3
O-901	Websterite (A)	28.1	69.2	2.7	
O-1085	Websterite (A)	57.5	40.4	2.1	
O-1101	Websterite (A)	39.3	56.1	4.6	
O-1109	Websterite (A)	37.6	57.7	4.7	
O-129/74	Peridotite				
O-1040	Peridotite				
O-1100	Peridotite				
O-1104	Peridotite				
O-1105	Peridotite				
O-1106	Peridotite				
O-1107	Peridotite				

12.5 mm. Clinopyroxene typically displays exsolution of orthopyroxene, ranging in width from 10 to 20 μm, along {100} crystallographic planes. Sample O-423 consists of a single, pale green, euhedral clinopyroxene crystal (> 5 cm). This large clinopyroxene poikilitically encloses numerous medium-grained, subhedral and elongate garnets which range between 1.5 and 6 mm. These garnets are mainly a product of exsolution, in which case this sample is technically a pyroxenite. The clinopyroxene also contains exsolution of fine-grained lamellae (1 to 5 μm wide) of orthopyroxene parallel to {100}. Varying amounts of rutile exsolution in garnets are also present along the {111} crystallographic planes in all eclogite samples. Numerous fine fractures cross-cutting the sample contain penetrating kimberlitic and carbonate materials. In spite of these fractures, the samples are relatively fresh, having experienced little secondary alteration, especially weathering.

All of the eclogites/websterite xenoliths contain a complex network of anastamosing fractures which are filled, to varying degrees, with kimberlitic material and variable amounts of metasomatic alteration products. The most common secondary minerals are chlorite/serpentine (?) and phlogopite. Selvages of phlogopite in association with kimberlite occur mantling many of the garnets in this suite, some present in kelyphitic rims. The garnets also show evidence of phlogopite growth along internal fractures which are penetrated by kimberlite. Trace amounts of small pyrrhotite grains, commonly mantled by rims of chalcopyrite, are associated only with the alteration products found in these kimberlite-filled fractures. Clinopyroxene is similarly altered along grain boundaries and internal fractures, with small, optically continuous "islands" of lower-Na clinopyroxene, set within a matrix of microcrystalline glass/plagioclase and spinel. These features have been called "spongy texture" by Taylor and Neal (1989), and are considered the product of partial melting of the primary clinopyroxene (Spetsius and Taylor 2002). Such features are common in all groups of eclogite xenoliths from kimberlites (e.g., Taylor and Neal 1989; Fung and Haggerty 1995; Snyder et al. 1998).

Analytical methods

Major- and minor-element compositions of minerals were determined with a Cameca SX-50 electron microprobe at the University of Tennessee. Analytical conditions employed an accelerating voltage of 15 keV, a beam current of 20 nA, beam size of 5 μm, and 20-s counting times for all elements, except K in clinopyroxene and Na in garnet (60-s each). All analyses underwent full ZAF (Cameca PAP) corrections. Trace-element concentrations were determined using secondary ion mass spectrometers—SIMS, Cameca IMS 4f at the University of New Mexico, and Cameca IMS 3f at the Woods Hole Oceanographic Institute. The operating procedures at both laboratories are approximately the same, and details about trace-element measurements by SIMS and analytical uncertainty have been presented by Shimizu et al. (1978) and Shimizu and Hart (1982).

Oxygen-isotope analyses of garnet were performed using a laser-fluorination technique at the University of Wisconsin-Madison. Samples were lightly crushed, and clean garnets were handpicked with a binocular microscope. The garnets were then crushed again, and

alteration products were removed again by picking, followed by an acid wash. Two samples (O-501 and O-927) were prepared using the thin-saw blade technique (Elsenheimer and Valley 1993). Thick sections (500–600 μm) were mounted on a glass slide with acetone-soluble, quick-setting cement and slightly polished prior to the thin-saw blade technique. Crowe et al. (1990) and Elsenheimer and Valley (1992, 1993) have described the laser extraction methodology used for oxygen-isotope analysis. Garnets were heated with a CO_2 laser beam $\sim$500 μm in diameter in the presence of $\sim$1,000 μmol BrF_5 and from an initial power density of 5×10^6 W/m^2, increasing to a final power density of 4.5×10^7 W/m^2.

For radiogenic-isotopic analysis, ultrapure mineral separates, hand-picked with a binocular microscope, were leached using a scheme modified from Zindler and Jagoutz (1988). Approximately 30 to 100 mg of sample was dissolved for each mineral-separate analysis. Techniques for chemical separation and mass spectrometric analysis of the isotopes of Rb, Sr, Sm, and Nd and isotope-dilution procedures are outlined in detail in Lee at al. (1993) and Snyder et al. (1994). Total-process blanks for chemical procedures were always less than 10 pg Rb, 120 pg Sr, 10 pg Sm, and 50 pg Nd. Sr and Nd isotopic data were obtained by multidynamic analysis with a VG Sector multicollector mass spectrometer at the University of Michigan. All Sr and Nd isotopic analyses are normalized to $^{86}Sr/^{88}Sr = 0.1194$ and $^{146}Nd/^{144}Nd = 0.7219$, respectively. Analyses of NIST-SRM 987 Sr and La Jolla Nd standards were performed throughout this study, and gave weighted averages (at the 95% confidence limit, external precision) of $^{87}Sr/^{86}Sr = 0.710250 \pm 0.000011$, and $^{143}Nd/^{144}Nd = 0.511854 \pm 0.000011$, respectively. Internal, within-run statistics are almost always of higher precision than the external errors. All isotope-dilution measurements utilized static-mode multicollector analyses. By convention, the Nd isotopic data are also presented in epsilon units, deviation relative to a chondritic uniform reservoir, CHUR (DePaolo and Wasserburg 1976):

$$\varepsilon_{Nd} = \left[\left(^{143}Nd/^{144}Nd_{sample} - {}^{143}Nd/^{144}Nd_{CHUR}\right)/{}^{143}Nd/^{144}Nd_{CHUR}\right] \times 10^4,$$
$$\text{where present} - \text{day}\left(^{146}Nd/^{144}Nd\right)_{CHUR} = 0.512638.$$

Due to the relatively small size of the xenoliths, and the difficulty in picking pure-mineral separates, there was often only one opportunity to generate data on a particular mineral separate. An analytical problem occurred during the analysis which did not allow Rb abundance measurements to be made. However, Rb is routinely low in garnet and clinopyroxene separates from Yakutian eclogites (e.g., Snyder et al. 1997), leading to exceedingly low $^{87}Rb/^{86}Sr$ ratios. In reality, due to the extremely low Rb abundances and low $^{87}Sr/^{86}Sr$ ratios expected, the age correction for $^{87}Sr/^{86}Sr$ is insignificant, at the time of the kimberlite emplacement.

Results

Mineral chemistry

In general, clinopyroxenes in eclogite xenoliths from kimberlites show systematic compositional variations (e.g., Taylor and Neal 1989). Clinopyroxenes in all the studied eclogites are compositionally zoned (i.e., heterogeneous), especially in Al_2O_3. Core-to-rim compositional variations include decreasing Al_2O_3, Na_2O, and FeO, and increasing MgO and CaO. Clinopyroxenes in samples O-501 and O-927 also show increased Cr_2O_3 from core to rim. With the exception of O-4, the clinopyroxenes in the websterites are also zoned similar to the eclogites. Major-element compositions of clinopyroxenes, along with other minerals, are summarized in Table 2.

Based on the MgO–Na_2O compositional relations of clinopyroxenes, eclogites can be subdivided into three groups (A, B, and C), as shown in Fig. 2 (after Taylor and Neal 1989). The distinction between B/C and A eclogites is also a function of lower Na_2O ($\sim$4 wt%), and higher Cr in those in group A (0.1–0.7 wt%). In Fig. 2, core compositions of clinopyroxenes from samples O-501 and O-82/91 plot in the group B field. These samples contain higher Al_2O_3 (8.7 and 8.4 wt%, respectively), higher Na_2O (4.8 and 4.5 wt%), lower MgO ($\sim$11 wt%), and lower Cr_2O_3 (0.04 and 0.08 wt%), compared to the rest of the suite. Sample O927 shows the same, group B, low-Cr chemical feature, although it plots in the group A field. For the clinopyroxene from the group A eclogites and the websterites, Cr_2O_3 contents are 0.11–0.54 wt%, which is in the range of compositions previously reported for group A eclogites (0.11–0.76 wt%; Sobolev 1977; Taylor and Neal 1989; Spetsius and Serenko 1990; Qi et al. 1994). These contents are significantly higher than those encountered in the group B and C eclogites from Mir and Udachnaya (Beard et al. 1996; Snyder et al. 1997). Clinopyroxenes in sample O-901 and sample O-86/91 of Qi et al. (1994) plot in the group B compositional field, but also contain significant amounts of Cr_2O_3 (0.10–0.54 wt%), more than "normal" group B eclogites. Because of these Cr_2O_3 contents, these xenoliths are considered to be akin to group A eclogites. In agreement with this consideration of the clinopyroxenes, garnets from these samples also plot in the group A region (Fig. 3).

In the group A eclogites and websterites, clinopyroxenes show transitional major-element compositions between the Udachnaya and Mir group B and C eclogites and those from the mantle peridotites. As expected, clinopyroxenes in the group B eclogites from

Table 2 Average major-element compositions of minerals in eclogite (*E*) and websterite (*W*) xenoliths from the Obnazhennaya kimberlite

Sample	**O-82/91 E**		**O-423 E**		**O-501 E**		**O-926 E**		**O-927 E**		**O-1073 E**	
	Cpx[a]	Gt	Cpx	Gt	Cpx	Gt	Cpx	Gt	Cpx	Gt	Cpx	Gt
# of Pts.	≥12	≥12	31	80	51	59	46	46	38	68	55	59
SiO_2	53.1 (6)[b]	39.7 (1)	53.2 (7)	41.5 (1)	53.9 (8)	40.0 (4)	54.6 (4)	41.2 (3)	54.2 (6)	40.2 (2)	54.6 (5)	40.7 (3)
Al_2O_3	8.39 (20)	22.8 (1)	9.01 (5)	23.4 (1)	8.68 (9)	22.5 (2)	6.38 (13)	23.2 (4)	7.34 (18)	22.8 (3)	3.86 (12)	23.0 (2)
TiO_2	0.35 (3)	0.08 (1)	0.05 (3)	0.03 (1)	0.34 (4)	0.11 (9)	0.14 (2)	0.05 (2)	0.26 (5)	0.06 (4)	0.11 (7)	0.07 (2)
Cr_2O_3	0.08 (3)	0.06 (3)	0.22 (3)	0.17 (6)	0.04 (4)	0.07 (2)	0.22 (4)	0.14 (5)	0.07 (2)	0.12 (2)	0.35 (4)	0.27 (8)
FeO	5.11 (20)	16.6 (1)	1.97 (5)	8.63 (6)	5.04 (6)	16.5 (3)	3.10 (8)	14.0 (3)	4.33 (6)	15.9 (5)	3.99 (8)	16.4 (6)
MnO	0.05 (3)	0.31 (3)	0.03 (1)	0.22 (3)	0.03 (2)	0.35 (8)	0.06 (2)	0.29 (4)	0.04 (2)	0.36 (7)	0.07 (3)	0.36 (4)
MgO	11.0 (4)	11.7 (1)	13.0 (7)	19.9 (2)	10.8 (8)	11.7 (4)	13.4 (2)	17.7 (6)	12.4 (4)	14.4 (3)	14.8 (4)	15.4 (6)
CaO	16.3 (4)	9.08 (1)	19.1 (4)	5.78 (5)	16.2 (6)	8.66 (9)	18.2 (4)	3.93 (6)	17.3 (7)	6.55 (2)	19.6 (3)	4.20 (4)
Na_2O	4.47 (12)	0.04 (1)	2.86 (6)	<0.03	4.76 (1)	<0.03	3.37 (9)	<0.03	3.84 (12)	<0.03	2.19 (9)	0.03 (1)
K_2O	n.a.	n.a.	<0.03	n.a.	<0.03	n.a.	<0.03	n.a.	<0.03	n.a.	<0.03	n.a.
Total	98.83	100.31	99.44	99.63	99.79	99.89	99.47	100.50	99.78	100.39	99.57	100.40
Mg#	0.795	0.559	0.922	0.806	0.794	0.561	0.886	0.695	0.838	0.620	0.870	0.628

Sample	**O-1103 E**		**O-1108 E**			**O-4 W**			**O-81/91 W**			**O-83/91 W**			**O-84/91 W**		
	Cpx	Gt	Cpx	Gt	Opx	Cpx	Gt	Opx	Cpx	Gt	Opx	Cpx	Gt	Opx	Cpx	Gt	Opx
# of Pts.	52	62	21	8	8	52	45	1	≥12	≥12	≥12	≥12	≥12	≥12	≥12	≥12	≥12
SiO_2	53.5 (4)	41.4 (3)	52.9 (4)	41.6 (3)	54.9 (5)	54.6 (3)	40.5 (2)	54.8	54.3 (2)	41.9 (2)	57.3 (1)	53.3 (4)	41.3 (3)	57.2 (1)	53.7 (2)	42.1 (3)	56.6 (2)
Al_2O_3	7.56 (14)	23.2 (2)	8.07 (92)	23.4 (2)	3.67 (12)	2.60 (4)	22.5 (1)	0.66	5.50 (31)	23.4 (1)	1.04 (18)	6.00 (25)	23.4 (1)	0.87 (4)	7.15 (20)	23.9 (2)	1.52 (12)
TiO_2	0.51 (5)	0.11 (3)	0.63 (5)	0.11 (3)	0.09 (1)	0.08 (2)	0.06 (1)	0.04	0.47 (3)	0.13 (2)	0.07 (2)	0.34 (2)	0.11 (2)	0.09 (2)	0.37 (4)	0.11 (2)	0.04 (1)
Cr_2O_3	0.11 (1)	0.12 (3)	0.63 (7)	0.59 (8)	0.18 (4)	0.33 (3)	0.52 (6)	0.06	0.37 (5)	0.34 (5)	0.07 (3)	0.17 (3)	0.21 (3)	0.05 (3)	0.27 (4)	0.32 (3)	0.05 (1)
FeO	3.26 (2)	11.9 (4)	2.28 (10)	9.94 (46)	6.94 (19)	4.11 (6)	17.3 (2)	12.8	2.66 (9)	10.4 (2)	6.26 (15)	3.05 (8)	10.9 (1)	6.54 (1)	1.69 (5)	7.35 (20)	6.50 (3)
MnO	0.08 (4)	0.33 (3)	0.06 (2)	0.38 (5)	0.13 (2)	0.10 (3)	0.45 (4)	0.13	0.04 (2)	0.27 (3)	0.06 (3)	0.05 (2)	0.25 (3)	0.05 (3)	0.04 (2)	0.29 (3)	0.05 (1)
MgO	12.7 (3)	18.9 (7)	12.8 (6)	19.7 (4)	33.2 (5)	15.7 (6)	14.5 (2)	30.2	14.1 (2)	19.8 (5)	34.8 (4)	13.9 (2)	19.7 (1)	34.1 (3)	14.0 (2)	21.9 (3)	33.9 (5)
CaO	17.8 (4)	4.10 (5)	18.0 (6)	4.27 (2)	0.20 (2)	20.9 (3)	4.57 (6)	0.41	19.0 (3)	4.16 (8)	0.41 (12)	19.0 (1)	4.26 (6)	0.23 (3)	19.3 (2)	4.28 (7)	0.22 (6)
Na_2O	3.79 (8)	0.04 (1)	3.66 (29)	0.04 (1)	0.05 (1)	1.53 (4)	<0.03	0.08	3.09 (12)	0.03 (1)	0.08 (3)	3.10 (10)	0.03 (1)	0.04 (1)	3.07 (9)	0.03 (1)	0.04 (1)
K_2O	<0.03	n.a.	<0.03	n.a.	<0.03	<0.03	n.a.	0.03	n.a.	n.a.	n.a.	n.a.	n.a.	n.a.	n.a.	n.a.	n.a.
Total	99.31	100.10	99.11	100.09	99.34	99.95	99.93	99.18	99.50	100.40	100.09	98.87	100.07	99.10	99.59	100.21	99.02
Mg#	0.875	0.741	0.910	0.781	0.896	0.873	0.601	0.809	0.905	0.774	0.909	0.891	0.765	0.904	0.937	0.843	0.904

Sample #	**O-85/91 W**			**O-86/91 W**			**O-901 W**		**O-1085 W**			**O-1101 W**			**O-1109 W**		
# of analysis	≥12	≥12	≥12	≥12	≥12	≥12	73	43	3	2	13	≥12	11	2	47	32	1
SiO_2	54.9 (3)	40.7 (3)	57.0 (2)	54.2 (2)	41.4 (1)	56.8 (3)	53.3 (8)	41.3 (3)	54.7 (3)	41.4 (2)	56.9 (1)	53.7 (7)	40.0 (4)	55.6 (1)	53.1 (4)	42.4 (3)	57.8
Al_2O_3	5.73 (12)	23.2 (2)	0.67 (3)	7.55 (22)	23.2 (1)	1.74 (10)	9.05 (18)	23.2 (4)	5.29 (57)	23.2 (1)	0.73 (7)	2.85 (0.58)	22.6 (2)	0.68 (2)	8.06 (16)	23.7 (5)	1.17
TiO_2	0.13 (1)	0.03 (2)	<0.03	0.47 (6)	0.11 (2)	0.03 (2)	0.47 (4)	0.13 (4)	0.25 (4)	0.07 (2)	0.05 (1)	0.11 (9)	0.06 (2)	0.04 (1)	0.66 (7)	0.10 (2)	0.09
Cr_2O_3	0.24 (2)	0.23 (3)	0.03 (1)	0.20 (2)	0.16 (3)	0.04 (2)	0.54 (11)	0.62 (6)	0.04 (1)	0.05 (1)	<0.03	0.33 (3)	0.48 (10)	0.18 (7)	0.29 (5)	0.28 (3)	0.14
FeO	3.06 (9)	15.0 (1)	9.37 (12)	3.38 (8)	12.6 (3)	6.21 (7)	3.00 (9)	11.0 (6)	3.44 (5)	13.3 (1)	8.54 (10)	4.39 (41)	16.7 (1)	12.5 (1)	1.77 (2)	7.71 (6)	4.44
MnO	0.04 (2)	0.36 (3)	0.09 (2)	0.06 (2)	0.33 (3)	0.04 (2)	0.07 (3)	0.33 (4)	0.03 (1)	0.22 (1)	0.06 (1)	0.08 (2)	0.40 (2)	0.08 (5)	0.03 (1)	0.28 (5)	0.07
MgO	13.6 (1)	17.1 (1)	32.7 (1)	12.4 (3)	19.8 (2)	33.9 (3)	11.8 (5)	19.7 (3)	13.7 (4)	17.8 (1)	33.0 (1)	15.6 (2)	15.2 (5)	30.0 (3)	13.5 (4)	21.8 (4)	36.7
CaO	18.4 (3)	3.92 (8)	0.21 (1)	16.9 (4)	3.82 (4)	0.32 (5)	16.3 (7)	3.98 (7)	18.7 (6)	4.00 (21)	0.23 (2)	20.7 (8)	4.56 (10)	0.46 (3)	18.4 (3)	4.10 (6)	0.2
Na_2O	3.29 (7)	<0.03	0.05 (1)	4.45 (12)	0.04 (1)	0.04 (2)	4.47 (18)	0.04 (1)	3.17 (29)	<0.03	0.05 (1)	1.52 (6)	<0.03	0.07 (1)	3.51 (7)	0.03 (1)	0.04
K_2O	n.a.	n.a.	n.a.	n.a.	n.a.	n.a.	<0.03	n.a.	<0.03	n.a.	<0.03	<0.03	n.a.	<0.03	<0.03	n.a.	0.03
Total	99.51	100.52	100.12	99.54	100.22	99.12	99.00	100.3	99.31	99.95	99.65	99.29	99.97	99.47	99.32	100.40	100.65
Mg#	0.889	0.672	0.863	0.868	0.739	0.908	0.876	0.763	0.878	0.707	0.874	0.865	0.620	0.812	0.932	0.836	0.937

[a]Cpx, clinopyroxene; gt, garnet; opx, orthopyroxene; n.a., not analyzed.
[b]The value in parentheses represents the one sigma precision of replicate analyses as expressed by the last digit cited

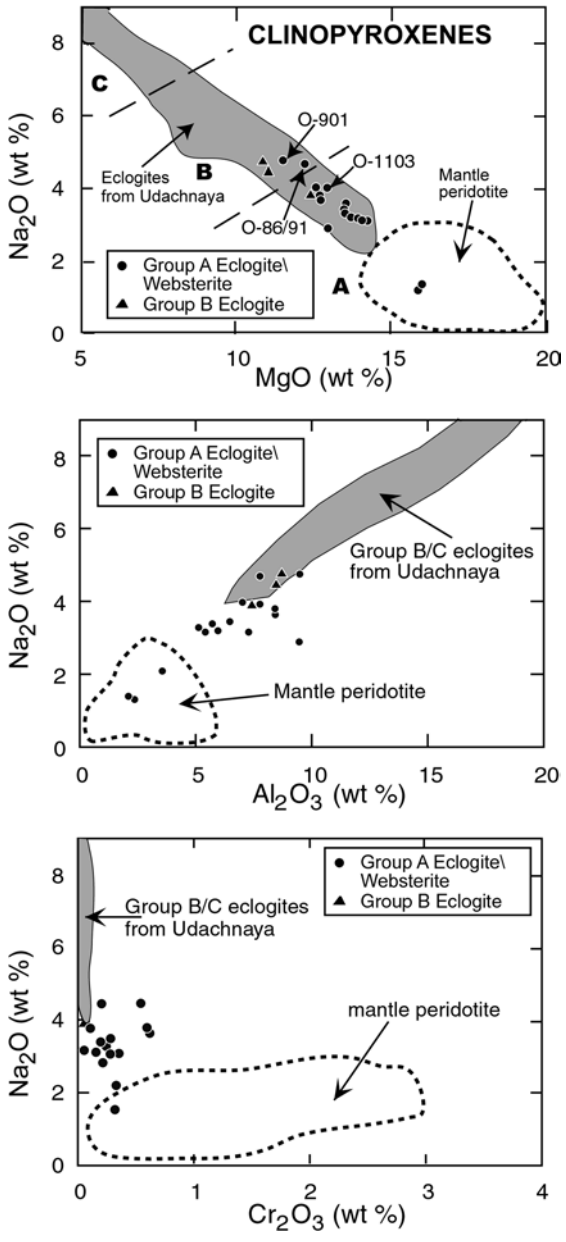

Fig. 2 Major-element compositional features of clinopyroxenes in eclogitic/websteritic xenoliths from the Obnazhennaya kimberlite. Note the comparison with those clinopyroxenes in the group *A*, *B*, and *C* eclogites from the Udachnaya pipe in Siberia (Jerde et al. 1993; Sobolev et al. 1994; Beard et al. 1996; Snyder et al. 1997) and those from mantle peridotites of worldwide occurrences (e.g., Sobolev 1977; Boyd 1989; Johnson et al. 1990; Hauri et al. 1993; Harris et al. 1994; Pearson et al. 1994; Stachel and Harris 1997a, 1997b; Coltorti et al. 1999; Xu et al. 2000; our unpublished data from Udachnaya peridotite xenoliths), as well as those from the Obnazhennaya kimberlite (Table 3). The subdivisions for eclogites into *A*, *B*, and *C* groups are after Taylor and Neal (1989)

Obnazhennaya plot in the range of the Udachnaya and Mir group B and C eclogites (Fig. 2). The Mg#s of clinopyroxenes in Udachnaya group B and C eclogites are 0.71–0.91 (Sobolev et al. 1994), with 0.90–0.98 for those in mantle peridotite. The studied clinopyroxenes in websterites and group A eclogites from Obnazhennaya have an intermediate Mg# range of 0.86–0.94. This intermediate compositional feature of the group A eclogites and websterites between the group B/C eclogites and peridotites (Table 3) is also obvious in the MgO–Na_2O, Al_2O_3–Na_2O, and Cr_2O_3–Na_2O plots, as shown in Fig. 2.

Garnet is one of the most important constituents of eclogite, and its chemical composition largely reflects the nature of the eclogite. Garnets from the studied eclogites and websterites exhibit intra- and intergrain homogeneity (Table 2), with the exception of samples O-501 and O-927. Group A garnets are MgO-rich, with a pyrope component of 60 to 75%. Contents of Cr_2O_3 are relatively high (0.12–0.62 wt%), except in sample O-1085 (0.05 wt%). Garnets from the group B eclogites O-501, O-927, and O-82/91 (Qi et al. 1994) have lower contents of MgO (43–51% pyrope) and Cr_2O_3 (0.06–0.12 wt%), in keeping with the group B classification criteria of Taylor and Neal (1989) and Taylor (1993). As shown in Fig. 3, garnets from three samples plot within the group B field (O-4 W, O-1073 E, and O-1101 W) but contain significant amounts of Cr_2O_3 (0.27–0.52 wt%), an indication of group A affinities. Samples O-4 W and O-1101 W are websterites, and sample O-1073 is an eclogite. Additionally, primary orthopyroxene exists in samples O-4 and O-1101. Therefore, these three samples are considered to be in group A. In Fig. 3, the group A garnets show intermediate nature between group B/C eclogite and peridotite, in terms of Ca–Mg–Fe composition. All these garnets, both group A and group B, are low in Na_2O contents (<0.03–0.05 wt%), compared with those in the group B/C diamondiferous eclogites from the Udachnaya kimberlite pipe (0.05–0.24 wt%; Sobolev and Lavrent'yev 1971; Sobolev et al. 1994, 1998b), and those from the Mir kimberlite pipe (0.07–0.17 wt%; Beard et al. 1996; Fig. 4). This is a direct function of the non-diamondiferous nature of the Obnazhennaya samples (Sobolev and Lavrent'yev 1971). In the garnet structure, Cr and Al occupy the same site. Thus, due to the limited Cr_2O_3 contents, Al_2O_3 contents in the studied garnets are much higher than those from peridotitic xenoliths and those from peridotitic garnet inclusions in diamonds (Fig. 4).

Orthopyroxene occurs as part of the primary assemblage in the ten websterite samples (Table 1). Comparison of granular groundmass orthopyroxene with the composition of exsolved orthopyroxene lamellae in clinopyroxene shows that some are compositionally distinct (Table 4). This implies that some of the granular orthopyroxene may be primary, and not necessarily the result of orthopyroxene exsolving and migrating from a clinopyroxene host, as suggested by Qi et al. (1994). Orthopyroxenes occurring as exsolution lamellae typically are more Al_2O_3- and FeO-rich than their discrete granular counterparts in the same samples. Primary orthopyroxenes are Mg-rich, with an enstatite component range between 81 and 92.7 mol%. Generally, orthopyroxenes are homogeneous, except in sample

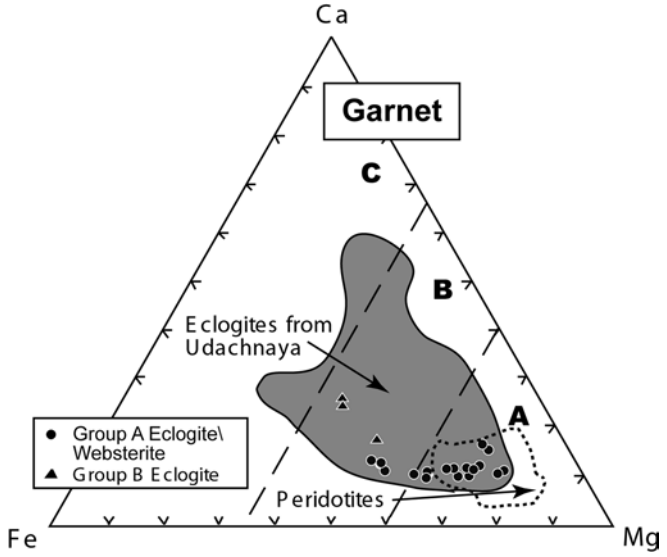

Fig. 3 Eclogitic and websteritic garnet compositions from Obnazhennaya. Garnets from Udachnaya eclogites are shown for comparison. Udachnaya group *A*, *B*, and *C* eclogite data are from Jerde et al. (1993), Sobolev et al. (1994), Beard et al. (1996), and Snyder et al. (1997, 1998). Peridotitic garnets shown here are mainly those in peridotite xenoliths from Udachnaya pipe and inclusions in diamonds (Sobolev 1977; Boyd et al. 1993; Pearson et al. 1994; our unpublished data from Udachnaya peridotite xenoliths), and those from the Obnazhennaya kimberlite (Table 3

O-1109, where they are slightly zoned in Al_2O_3 (core-to-rim, 1.17 to 0.85 wt% Al_2O_3).

Chlorite and phlogopite are found replacing primary minerals along grain boundaries and fractures. Both hydrous phases are the result of interaction between fluids and the host eclogites. The presence of phlogopite as part of the kelyphitic rims mantling many of the garnets in these samples requires a K-rich metasomatic fluid or melt to have interacted with the garnets, since garnets contain $< < 1$ wt% K_2O (Hunter and Taylor 1982). This fluid could be kimberlitic, also responsible for the partial melting which created the secondary phases in the clinopyroxene spongy textures in the eclogites (Spetsius and Taylor 2002).

Equilibrium pressure and temperature

Equilibrium pressures and temperatures for both garnet peridotite and the websterites were estimated using clinopyroxene–orthopyroxene, Fe–Mg exchange, and the Al_2O_3 solubility in orthopyroxene, according to the calibrations of Brey and Köhler (1990). Olivine basically does not appear in the group A eclogites. However, the geothermometer and geobarometer are still applicable, because this does not affect the element partitioning between clinopyroxene–orthopyroxene and garnet–orthopyroxene. Additionally, as shown by Sobolev et al. (1999), it is not possible to accurately calculate Fe^{3+} from electron microprobe analyses. Therefore, all Fe in clinopyroxene and garnet is

Table 3 Average major-element compositions of minerals in peridotite xenoliths from the Obnazhennaya kimberlite

Sample	O-1104				O-1105				O-1106				O-1107				O-127/94				O-1040				O-1100			
# of Pts.	Cpx[a] 7	Gt 10	Opx 3	Ol 2	Cpx 7	Gt 8	Opx 5	Ol 8	Cpx 10	Gt 4	Opx 18	Ol 5	Cpx 24	Gt 21	Opx 11	Ol	Cpx 10	Gt 6	Opx 10	Ol 4	Cpx 13	Opx 4	Ol 10	Cpx 9	Opx 7	Ol 4
SiO_2	53.6 (5)[b]	42.2 (4)	57.7 (9)	40.8 (1)	54.2 (4)	41.4 (7)	57.5 (2)	40.7 (3)	53.9 (3)	41.9 (1)	57.7 (5)	41.1 (2)	53.9 (5)	42.3 (3)	57.9 (4)	41.8 (2)	53.3 (4)	41.8 (2)	56.2 (4)	41.1 (1)	52.2 (5)	55.0 (6)	40.5 (4)	52.8 (5)	56.0 (7)	40.3 (3)
Al_2O_3	4.16 (14)	22.9 (4)	1.51 (3)	< 0.03	3.22 (19)	20.8 (6)	0.89 (7)	< 0.03	7.24 (90)	22.0 (1)	1.30 (47)	n.a.	4.09 (56)	22.7 (3)	1.31 (27)	4.09 (90)	22.2 (3)	1.86 (31)	< 0.03	3.88 (40)	3.60 (7)	< 0.03	5.68 (42)	2.83 (24)	< 0.03	
TiO_2	0.27 (6)	0.08 (1)	0.09 (3)	< 0.03	0.13 (4)	0.13 (4)	0.06 (2)	< 0.03	0.49 (7)	0.09 (2)	0.11 (2)	n.a.	0.50 (9)	0.10 (2)	0.09 (2)	0.31 (12)	0.09 (3)	0.08 (1)	< 0.03	< 0.03	< 0.03	< 0.03	< 0.03	0.25 (3)	0.05 (2)	< 0.03
Cr_2O_3	0.85 (4)	1.17 (4)	0.30 (5)	0.02 (1)	2.20 (11)	4.14 (60)	0.32 (4)	< 0.03	2.09 (20)	2.14 (9)	0.40 (18)	n.a.	1.59 (28)	2.00 (31)	0.34 (6)	1.37 (9)	2.20 (51)	1.18 (4)	< 0.03	1.31 (23)	0.74 (21)	< 0.03	2.01 (6)	0.46 (8)	n.d.	
FeO	1.52 (11)	7.28 (24)	4.17 (11)	6.63 (1)	2.09 (28)	6.80 (80)	4.41 (8)	7.43 (11)	1.50 (18)	8.39 (56)	4.62 (12)	7.56 (18)	1.11 (6)	6.36 (31)	3.60 (15)	1.81 (21)	7.58 (50)	4.87 (29)	7.26 (9)	1.74 (32)	5.11 (22)	8.12 (9)	1.69 (10)	4.95 (11)	8.07 (72)	
NiO	n.a.	n.a.	n.a.	0.44 (1)	n.a.	n.a.	n.a.	0.34 (3)	n.a.	n.a.	n.a.	0.45 (5)	n.a.	n.a.	n.a.	n.a.	n.a.	n.a.	n.a.	0.42 (4)	n.a.	n.a.	0.39 (4)	n.a.	n.a.	0.39 (4)
MnO	0.04 (1)	0.30 (3)	0.08 (2)	0.09 (2)	0.06 (2)	0.40 (8)	0.11 (2)	0.12 (1)	0.06 (2)	0.41 (8)	0.09 (2)	0.08 (3)	0.03 (2)	0.28 (5)	0.07 (3)	0.05 (1)	0.38 (6)	0.11 (2)	0.08 (2)	0.08 (2)	0.13 (3)	0.12 (2)	0.07 (2)	0.11 (4)	0.11 (1)	
MgO	15.9 (7)	21.3 (4)	35.9 (6)	52.0 (1)	15.3 (2)	21.0 (9)	36.5 (2)	51.7 (5)	12.8 (9)	20.9 (3)	35.6 (6)	51.3 (1)	15.2 (3)	21.8 (4)	36.7 (3)	17.0 (6)	20.5 (2)	35.5 (4)	51.5 (1)	16.5 (9)	33.6 (6)	50.2 (4)	14.0 (2)	35.2 (7)	50.6 (6)	
CaO	21.5 (5)	4.80 (11)	0.47 (3)	< 0.03	19.5 (6)	5.30 (5)	0.25 (1)	< 0.03	18.1 (9)	4.33 (34)	0.27 (12)	< 0.03	20.9 (2)	4.83 (10)	0.21 (2)	19.4 (7)	5.00 (29)	0.35 (9)	< 0.03	22.4 (9)	0.95 (6)	< 0.03	19.1 (4)	0.33 (9)	< 0.03	
Na_2O	1.84 (31)	0.02 (1)	0.05 (2)	< 0.03	2.72 (26)	0.04 (1)	0.09 (1)	< 0.03	3.77 (60)	0.04 (2)	0.06 (3)	n.a.	2.25 (12)	0.03 (1)	0.04 (1)	1.85 (33)	< 0.03	0.05 (1)	n.d.	0.73 (6)	0.03 (3)	< 0.03	3.06 (23)	0.08 (4)	< 0.03	
K_2O	< 0.03	n.a.	< 0.03	< 0.03	< 0.03	n.a.	< 0.03	< 0.03	< 0.03	n.a.	< 0.03	n.a.	< 0.03	n.a.	< 0.03	0.03 (1)	n.a.	< 0.03	< 0.03	< 0.03	< 0.03	< 0.03	< 0.03	< 0.03	< 0.03	< 0.03
Total	99.71	100.10	100.16	100.02	99.53	100.00	100.22	100.30	99.99	100.28	100.13	100.50	99.60	100.42	100.26	99.14	99.84	100.19	100.40	98.85	99.21	99.36	98.62	99.97	99.53	
Mg#	0.950	0.841	0.939	0.934	0.930	0.848	0.937	0.926	0.939	0.818	0.933	0.924	0.961	0.861	0.948	0.944	0.830	0.929	0.927	0.945	0.922	0.917	0.937	0.928	0.919	

[a]Cpx, clinopyroxene; gt, garnet; opx, orthopyroxene; ol, olivine; n.a., not analyzed; n.d., not detected.
[b]The value in parentheses represents the one sigma precision of replicate analyses as expressed by the least digit cited

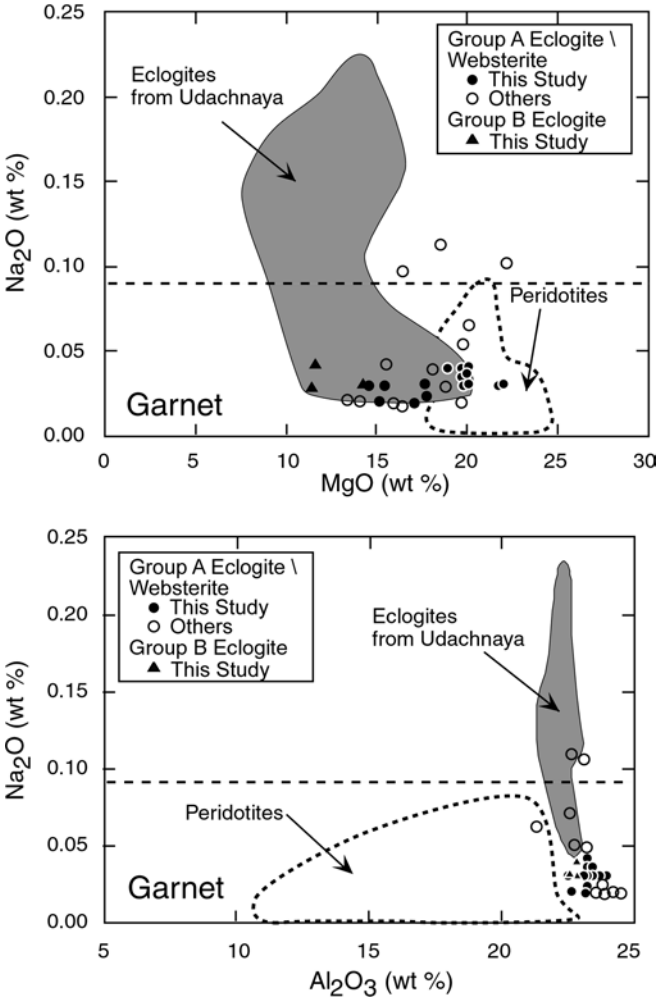

Fig. 4 Major-element compositions of garnets in eclogitic xenoliths from the Obnazhennaya. Note the comparison with the eclogites from the Udachnaya kimberlite (Sobolev et al. 1994; Snyder et al. 1997) and the peridotitic garnets from the same sources as in Fig. 3. Additional eclogite/websterite data are from Ouchinnikov (1989) and Ukhanov et al. (1988). Garnets in peridotite xenoliths from the Obnazhennaya kimberlite (Table 3) are also included

assumed to be Fe^{2+}. With this assumption, the temperature estimates reported herein are considered to represent maximum equilibration temperatures. Pressures will also be maxima. Nevertheless, if the same thermometer or barometer is applied to all the rocks, the uncertainties in comparison arise mainly from the precision of the EMP analyses.

Except for one garnet peridotite (O129/74) which shows relatively high P–T (41.6 kbar, 1,101 °C), the estimated pressures are from 21.0 to 37.6 kbar, and the temperatures from 711 to 923 °C, as shown in Fig. 5. Basically, no systematic differences between the websterite and peridotite groups were detected. This can be interpreted as indicating that all these xenoliths, including the group A and B eclogites/websterites and the peridotites, were captured by the ascending kimberlitic melt from the same general locality within the upper mantle. Overall, the results of these estimations

Table 4 Major-element compositions of orthopyroxenes in websterites (*W*) and exsolution lamellae in eclogites (*E*)

Part	Core	Rim	Core	Core	Core	Core	Core	Rim	Exsolution	Core	Core	Core	Rim	Exsolution	Exsolution	Exsolution	Exsolution
Sample	O-4 W		O-81/91 W	O-83/91 W	O-84/91 W	O-85/91 W	O-86/91 W	O-901 W			O-1085 W	O-1101 W	O-1109 W		O-926 E	O-1103 E	O-1108 E
SiO_2	54.8	55.0	57.3	57.2	56.6	57.0	56.8	56.1	56.3	55.0	56.9	55.6	57.8	58.1	55.3	56.6	56.2	54.9
Al_2O_3	0.66	0.66	1.04	0.87	1.52	0.67	1.74	1.18	1.01	3.47	0.73	0.68	1.17	0.85	3.46	0.76	1.97	3.67
TiO_2	0.04	0.03	0.07	0.09	0.04	< 0.03	0.03	0.06	0.10	0.07	0.05	0.04	0.09	0.12	0.07	0.03	0.08	0.09
Cr_2O_3	0.06	0.03	0.07	0.05	0.05	0.03	0.40	0.14	0.13	0.14	0.01	0.18	0.14	0.07	0.08	0.05	0.04	0.18
FeO	12.8	12.7	6.26	6.54	6.50	9.37	6.21	6.77	6.75	7.53	8.54	12.5	4.44	4.43	5.25	9.15	8.00	6.94
MnO	0.13	0.14	0.06	0.05	0.05	0.09	0.04	0.09	0.08	0.11	0.06	0.08	0.07	0.06	0.10	0.07	0.11	0.13
MgO	30.2	30.1	34.8	34.1	33.9	32.7	33.9	34.6	34.9	32.9	33.0	29.9	36.7	36.9	35.4	32.6	32.5	33.2
CaO	0.41	0.44	0.41	0.23	0.22	0.21	0.32	0.24	0.25	0.20	0.23	0.46	0.20	0.23	0.20	0.23	1.29	0.20
Na_2O	0.08	0.05	0.08	0.04	0.04	0.05	0.04	0.05	0.04	0.07	0.05	0.07	0.04	0.04	0.06	0.06	0.25	0.05
K_2O	< 0.03	< 0.03	n.a.	n.a.	n.a.	n.a.	n.a.	< 0.03	< 0.03	< 0.03	< 0.03	< 0.03	< 0.03	< 0.03	< 0.03	< 0.03	< 0.03	< 0.03
Total	99.18	99.15	100.09	99.10	99.02	100.12	99.12	99.23	99.56	99.49	99.65	99.47	100.65	100.80	99.92	99.55	100.44	99.34
Mg#	0.809	0.810	0.909	0.904	0.904	0.863	0.908	0.902	0.903	0.887	0.874	0.812	0.937	0.937	0.924	0.865	0.880	0.896

[a] *n.a.* (not analyzed)

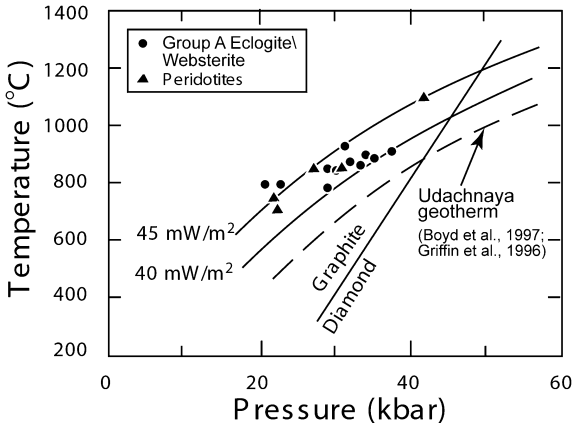

Fig. 5 Results of pressure and temperature estimations for Obnazhennaya xenoliths of both the group A eclogites/websterites and the garnet peridotites. All samples fall within the graphite stability field, consistent with the non-diamondiferous nature of the xenoliths and kimberlite. Note that the array of Obnazhennaya xenoliths appear to fall along a higher geotherm than that determined by Boyd et al. (1997) and Griffin et al. (1996) for the lithospheric mantle beneath Udachnaya. This difference is interpreted to be a function of the relative proximity of the Obnazhennaya pipe to the edge of the Siberian craton, compared to the central location for Udachnaya

show that all of the xenoliths from Obnazhennaya formed within the graphite stability field, a fact consistent with the barren nature for diamond of these xenoliths and host kimberlite. Estimations using the single-pyroxene geothermobarometer of Mercier (1976, 1980) give unreasonably low pressures (0–20 kbar) and temperatures (540–800 °C). This confirmed the arguments of Finnerty and Boyd (1984) and Nimis and Taylor (2000) that Mercier's single-pyroxene geothermobarometer probably gives erroneous results.

In contrast to xenoliths from Obnazhennaya, those from the Udachnaya and Mir kimberlites contain diamonds, and pressure estimations for these xenoliths are mostly above 40 kbar, some 10–20 kbar higher than for most from Obnazhennaya (Boyd et al. 1997). Similar conclusions about the mantle geotherm at Udachnaya were also reached by Griffin et al. (1996), by studying garnet xenocrysts in kimberlites. As shown in Fig. 5, our P–T estimations correspond to a mantle geotherm of 40–45 mW/m^2 at Obnazhennaya, definitely higher than that for the mantle beneath Udachnaya. This is probably related to the location of Udachnaya at the center of the Siberian platform, near the keel of the craton, whereas Obnazhennaya is near the edge (i.e., more shallow).

Trace-element geochemistry

Trace elements, particularly the rare-earth elements (REEs), in minerals from mantle xenoliths are very sensitive to the involved mantle processes during their formation, and thus may efficiently constrain these processes. In this study, 13 eclogite/websterite and

Table 5 Concentrations of rare-earth elements in minerals from xenoliths from the Obnazhennaya kimberlite (ppm)

Sample	O-82/91 E[a]		O-501 E		O-927 E		O-1073 E		0-4 W			0-1109 W	O-81/91 W		O-83/91 W		O-84/91 W		O-85/91 W		O-86/91 W		O-129/74 P			O-1105 P	
	Cpx	Gt	Cpx	Gt	Cpx	Gt	Cpx	Gt	Cpx	Gt	Opx	Gt	Cpx	Gt	Cpx	Cpx	Cpx	Gt	Cpx	Gt	Cpx	Gt	Cpx	Gt	Opx	Cpx	Gt	Opx
La	0.93	<0.02	2.33	0.06	3.69	0.04	0.84	<0.02	1.28	<0.02	<0.02	<0.02	1.08	n.a.	1.52	1.52	3.33	n.a.	0.34	n.a.	1.03	n.a.	2.85	0.03	0.54	2.85	0.03	0.54
Ce	4.39	0.31	7.40	0.34	14.9	0.38	1.37	0.11	2.60	0.03	<0.02	0.027	4.77	<0.02	5.61	5.61	18.1	0.04	1.52	<0.02	3.76	<0.02	11.6	0.05	0.88	11.6	0.05	0.88
Nd	4.17	1.08	4.06	0.68	9.26	0.99	1.63	0.14	1.81	0.15	0.049	0.556	6.02	0.24	5.04	5.04	22.7	1.63	1.67	0.07	5.84	0.20	7.67	0.61	0.21	7.67	0.61	0.21
Sm	1.19	0.83	1.00	0.52	2.23	0.92	0.84	0.34	0.83	0.39	0.069	1.09	2.16	0.68	1.31	1.31	6.46	2.35	0.57	0.17	2.88	0.65	1.67	0.94	0.08	1.67	0.94	0.08
Eu	0.37	0.59	0.35	0.47	0.70	0.56	0.43	0.28	0.37	0.26	0.02	0.654	0.90	0.43	0.53	0.53	1.89	1.17	0.26	0.12	1.17	0.55	0.55	0.45	0.03	0.55	0.45	0.03
Gd	0.94	n.a.	n.a.	n.a.	n.a.	n.a.	n.a.	n.a.	n.a.	n.a.	n.a.	n.a.	1.69	n.a.	1.02	1.02	5.05	n.a.	0.52	n.a.	2.42	n.a.	n.a.	n.a.	n.a.	n.a.	n.a.	n.a.
Dy	0.37	1.65	0.33	1.71	0.82	3.05	0.41	2.01	0.55	3.34	0.05	6.01	0.60	1.93	0.34	0.34	1.83	7.50	0.33	1.71	1.19	4.27	0.69	3.85	0.03	0.69	3.85	0.03
Er	0.14	1.13	n.a.	n.a.	n.a.	n.a.	n.a.	n.a.	n.a.	n.a.	n.a.	n.a.	0.20	1.10	0.13	0.13	0.61	6.34	0.13	1.65	0.39	2.61	n.a.	n.a.	n.a.	n.a.	n.a.	n.a.
Yb	n.a.	1.11	0.11	1.42	0.19	2.62	0.10	1.45	0.13	2.80	0.04	4.55	0.13	1.26	0.08	0.08	0.48	7.04	0.09	1.80	0.29	3.04	0.18	2.90	0.01	0.18	2.90	0.01

[a]E, eclogite; W, websterite; P, peridotite; cpx, clinopyroxene; gt, garnet; opx, orthopyroxene; n.a., not analyzed

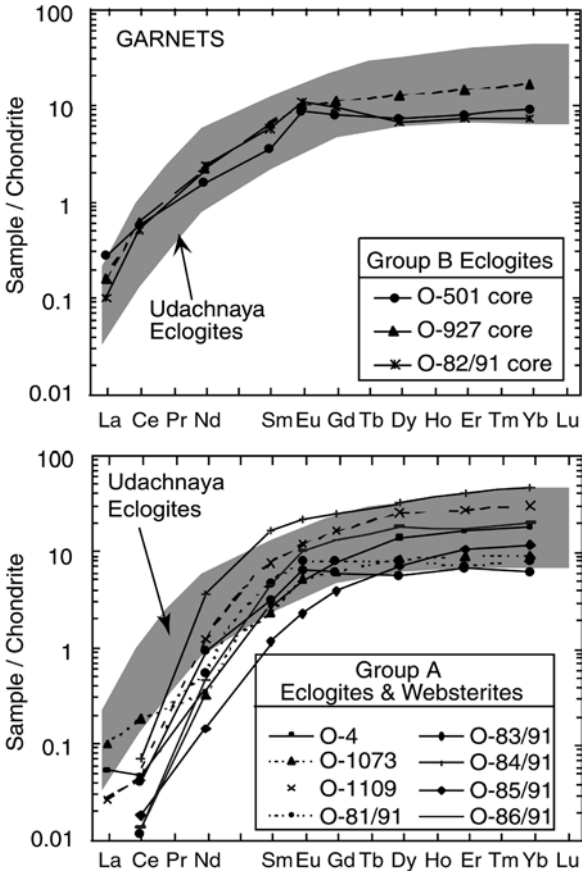

Fig. 6 Chondrite-normalized REE patterns of garnets from the Obnazhennaya kimberlite. Garnets in the eclogites from the Udachnaya kimberlite pipe are shown for comparison (*shaded area*; Jerde et al. 1993; Sobolev et al. 1994). All garnets of the group B and some from the group A eclogites show +Eu anomalies, albeit not large. Chondrite concentrations of REEs of McDonough and Sun (1995) were used for normalization

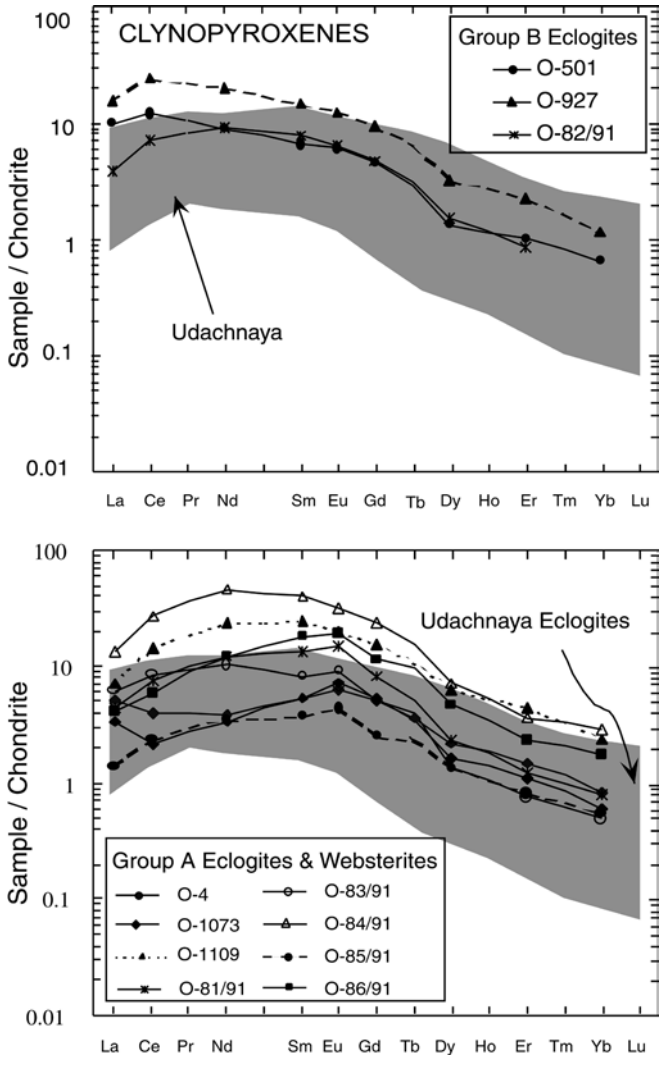

Fig. 7 Chondrite-normalized REE patterns of clinopyroxenes from the Obnazhennaya kimberlite. Clinopyroxenes in the eclogites from the Udachnaya kimberlite pipes are shown for comparison (*shaded area*; Jerde et al. 1993; Sobolev et al. 1994)

peridotite xenoliths from Obnazhennaya were analyzed for concentrations of REEs in garnet and clinopyroxene. The analytical results are summarized in Table 5.

Garnets from the three group B eclogites show typical, depleted chondrite-normalized REE patterns, with La_n of 0.10–0.61 and Yb_n of 7.0–16.5 (Fig. 6). They fall almost entirely within the range of garnets in the group B eclogite xenoliths from the Udachnaya pipe (Jerde et al. 1993; Ireland et al. 1994; Taylor et al. 1996, 1998, 2000), with $(La/Yb)_n$ of 0.01–0.05. Each of the three garnets show slight to medium positive Eu anomalies, where the ratios of Eu/Eu* are 1.2–1.5. By contrast, this anomaly was not detected from most of the xenoliths from Udachnaya (e.g., Jerde et al. 1993).

A distinguishing feature of garnets from the group A eclogites is the low concentrations of LREEs. Except for sample O-1073, the other samples are outside the range of Udachnaya group B/C eclogites, with La_n as low as 0.01–0.10. Concentrations of MREEs and HREEs increase distinctly with increasing atomic number, and the concentrations of HREEs are comparable with those in the group B/C eclogites from Udachnaya, as shown in Fig. 6. The Yb_n values vary between 6.0 and 44.2. Garnets from one group A eclogites and two group A websterites show positive Eu anomalies (O-1073, O-81/91, O-83/91), with Eu/Eu* of 1.2–1.4. This is similar to the diamond inclusions reported by Aulbach et al. (2002).

REE patterns of clinopyroxenes are shown in Fig. 7, in comparison with those in the group B/C eclogites from the Udachnaya and Mir kimberlites. Clinopyroxenes from the three group B Obnazhennaya eclogites exhibit convex-upward LREE patterns, with La_n of 3.9–17.9 and $(La/Yb)_n$ of 9.4–24.8. Sample O-927 is rich in LREEs and above the range of clinopyroxenes in the group B/C eclogites from the Udachnaya and Mir kimberlite. In contrast to the garnets of the same group, no evident Eu anomaly was detected in these clinopyroxenes. Clinopyroxenes in the group A eclogites exhibit much larger variations in both REE concentrations and shape of the patterns (Fig. 7). Both convex-upward and

Table 6 Oxygen-isotope analyses (δ^{18}O SMOW) of garnets from Obnazhennaya eclogites (*E*) and websterites (*W*)

Sample	Core	Rim
O-82/91 E	7.81	
O-423 E	6.07	
O-501 E	7.06	7.30
O-926 E	5.60	
O-927 E	6.32	6.30
O-1073 E	6.46	
O-1103 E	6.36	
O-4 W	6.35	
O-81/91 W	5.67	
O-83/91 W	5.46	
O-84/91 W	5.68	
O-85/91 W	5.51	
O-86/91 W	6.30	
O-901 W	5.79	
O-1109 W	6.14	

simple-enrichment patterns are present. Some samples have their highest contents in the MREEs. Portions of the samples are even above the range of group B/C eclogites, with La_n of 1.5–10.3 and $(La/Yb)_n$ of 2.4–15.9. Clinopyroxenes in the group A eclogites from southern Africa show much larger ratios of $(La/Yb)_n$ (130–270; Shervais et al. 1988). Except for clinopyroxenes in O-1109 and O-84/91, all others show + Eu anomalies, with Eu/Eu* between 1.2 and 1.9.

Oxygen isotopes

Oxygen isotopes of eclogites can retain crustal signatures from their protoliths. The oxygen-isotopic compositions of garnet were determined for 15 of the samples, and the results are summarized in Table 6 and

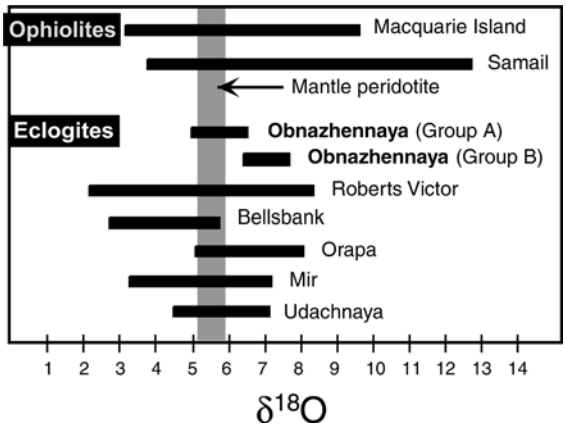

Fig. 8 Oxygen-isotopic compositions of garnets from Obnazhennaya eclogites, in comparison with ophiolites and eclogites from other occurrences. The mantle range indicated is from Mattey et al. (1994). Garnets from all group B eclogites and part of the group A eclogite/websterite suite have values outside the mantle range. Data are from Gregory and Taylor (1981), Cocker et al. (1982), MacGregor and Manton (1986), Neal et al. (1990), Jacob et al. (1994), Beard et al. (1996), Viljoen et al. (1996), and Snyder et al. (1997)

Fig. 8. Oxygen-isotopic compositions of ophiolites and eclogites of other occurrences are also plotted for comparison. Two samples were tested for possible compositional zonation; it was found that garnet in sample O-501 is slightly zoned, with δ^{18}O values of 7.06 at the core and 7.3 at the rim of one garnet grain. Garnets in the three group B eclogites from this suite (O-82/91, O-501, and O-927) have δ^{18}O values (6.3–7.81‰) which are well above the mantle range of Mattey et al. (1994; 5.5 ± 0.4‰). The majority of garnets from the other group A eclogites analyzed in this study are also above the mantle oxygen-isotope range,

Table 7 Isotopic composition of minerals and reconstructed whole rocks from Obnazhennaya websterites

Sample	Rb (ppm)	Sr (ppm)	$^{87}Rb/^{86}Sr$	$^{87}Sr/^{86}Sr$	Sm (ppm)	Nd (ppm)	$^{147}Sm/^{144}Nd$	$^{143}Nd/^{144}Nd$	Reference
Clinopyroxene									
O-81/91 cpx	(0.1)	306	0.00095	0.703447 ±23	2.48	7.96	0.188	0.512775 ±11	This study
O-81/91 ex/cpx	(0.1)	273	0.00106	0.703399 ±18	2.29	7.28	0.190	0.512647 ±12	This study
O-84/91 cpx	(0.1)	486	0.00060	0.703797 ±27	6.04	25.3	0.144	0.511572 ±09	This study
47637 cpx					1.02	6.07	0.102	0.511936 ±30	McCulloch (1989)
Yak-2 cpx					0.29	1.65	0.106	0.511941 ±32	McCulloch (1989)
Garnet									
O-81/91 rut–gt	(0.01)	4.99	0.00580	0.703684 ±20	0.66	0.48	0.821	0.517222 ±13	This study
O-84/91 gt	(0.01)	2.70	0.01070	0.704363 ±34	1.81	1.12	0.979	0.518356 ±09	This study
47637 gt					0.40	0.82	0.295	0.512787 ±30	McCulloch (1989)
Yak-2 gt					0.24	0.66	0.220	0.513176 ±40	McCulloch (1989)
Others									
O-84/91 serp	(0.01)	10.6	0.00273	0.703975 ±20	0.11	0.43	0.155	0.512144 ±12	This study
O-84/91 opx	6.20	52.3	0.34300	0.703861 ±13	0.94	3.79	0.149	0.511769 ±13	This study
Reconstructed whole rocks									
O-81/91	0.06	138	0.00126	0.70345 ±3	1.46	3.78	0.234	0.51309 ±2	
O-84/91	0.04	241	0.00048	0.70380 ±4	3.73	13.0	0.173	0.51181 ±2	
47637					0.71	3.45	0.124	0.51204 ±4	
Yak-2					0.27	1.16	0.138	0.51229 ±5	

Mineral proportions used for reconstructions (from Qi et al. 1994): O-81 = 55.9% garnet + 44.1% "cpx" (= "cpx" + "exsolved cpx"); O-84 = 39.4% garnet + 47.9% cpx + 12.5% opx

with some of them falling within the accepted mantle range. This shows that most of the group A eclogite xenoliths from the Obnazhennaya kimberlite have $\delta^{18}O$ values distinctly outside the mantle range. Qi et al. (1994) studied a suite of eclogite xenoliths from Obnazhennaya, composed of five group A websterites (O-81/91, O-83/91, O-84/91, O-85/91, and O-86/91) and one group B eclogite (O-82/91). Only two of their samples have $\delta^{18}O$ values above the mantle range. These include the group A websterite O-86/91 (6.3‰) and the group B eclogite O-82/91 (7.8‰).

Ustinov et al. (1987) determined $\delta^{18}O$ of 11 eclogite/websterite xenoliths from the Obnazhennaya kimberlite, including those in both groups A and B. For garnets from group A eclogites/websterites, $\delta^{18}O$ ranged from 6.8 to 7.0 ‰, with 5.4 to 7.0‰ for garnets from the group B eclogites. As in our study, these values of garnets in the group A eclogites/websterites are clearly above the mantle range and are consistent with those obtained in the present investigation. Additionally, oxygen in minerals from two peridotite xenoliths from the Obnazhennaya kimberlite were also determined by Ustinov et al. (1981); garnets and olivines have $\delta^{18}O$ values of 5.0–6.2‰, which are generally close to the mantle values. However, the values for clinopyroxenes and orthopyroxenes in these rocks were much lower (2.9–3.6‰). The large differences between garnet and pyroxenes are not a result of equilibrium isotopic fractionation. In summary, most of the eclogites and websterites studied from Obnazhennaya have oxygen isotopic evidence that their protoliths were crustally derived.

Nd and Sr isotopic composition

Mineral separates from two samples were analyzed for radiogenic isotopic compositions; the results are summarized in Table 7, together with the two samples analyzed by McCulloch (1989). Mineral separates from websterite sample O-81/91 are impure, with complexly exsolved clinopyroxene containing abundant garnet, and garnet containing abundant rods of rutile (labeled "rut–gnt" in Table 2). Two different clinopyroxene separates were analyzed from O-81/91, one containing less than 10 vol% garnet (labeled "cpx" in Table 7), and another with approximately 20–30 vol% garnet (labeled "ex/cpx" in Table 7). We were not able to analyze a "clean" orthopyroxene separate in O-81/91 but did so for websterite sample O-84/91. A chlorite mineral separate from O-84/91 was also analyzed.

The Nd and Sr isotopic compositions of mineral separates in websterite O-81/91 offer a confounding set of data. The garnet separate has the highest $^{87}Sr/^{86}Sr$ (0.703684 ±20) when compared to the clinopyroxene separates labeled "cpx" (0.703447 ±23) and "ex/cpx" (0.703399 ±18). However, the clinopyroxene separate with the largest proportion of exsolved garnet does not have a more elevated $^{87}Sr/^{86}Sr$, as might be expected from the relatively radiogenic nature of the garnet separate. Although the clinopyroxene separate with the largest proportion of exsolved garnet, "ex/cpx", has slightly lower Sm and Nd abundances than "cpx", the $^{147}Sm/^{144}Nd$ ratios of the two separates are virtually indistinguishable. In addition, the $^{143}Nd/^{144}Nd$ ratios of these two clinopyroxene separates are similar, with O-81/91 "cpx" having a ratio of 0.512775 ±11, and O-81/91 "ex/cpx" having a ratio of 0.512647 ±12. This could lead one to conclude that the garnet is not causing the difference in $^{143}Nd/^{144}Nd$ isotopic composition. However, an analysis of a garnet separate (enclosing exsolution rutile) in this sample yields a $^{143}Nd/^{144}Nd$ ratio of 0.517222 ±13. Either the rutile in this garnet has a very low amount of Nd with very high $^{143}Nd/^{144}Nd$, and/or garnet grains in the matrix of the rock have a vastly different $^{143}Nd/^{144}Nd$ than those exsolved from clinopyroxene. This is an area for further research with more appropriate samples.

The data from mineral separates in websterite O-84/91 are equally difficult to explain. As with O-81/91, the garnet separate in O-84/91 has the highest $^{87}Sr/^{86}Sr$ (0.704363 ± 34), when compared to clinopyroxene (0.703797 ± 27), chlorite (serpentine?) (0.703975 ±20), and orthopyroxene (0.703861 ±13). Although the $^{147}Sm/^{144}Nd$ ratios of clinopyroxene, serpentine/chlorite, and orthopyroxene are similarly LREE-enriched (0.144 to 0.155), the $^{143}Nd/^{144}Nd$ ratios are vastly different — 0.511572 ±09, 0.512144 ±12, and 0.511769 ±13, respectively. The garnet separate is the most LREE-depleted analyzed ($^{147}Sm/^{144}Nd$ = 0.979), and has a commensurately elevated $^{143}Nd/^{144}Nd$ ratio of 0.518356 ± 09. These data show that the garnets in both websterites, O-81/91 and O-84/91, are more radiogenic than other minerals in terms of Nd and Sr isotopes. Such a relationship is the norm for eclogites from both the Udachnaya (Snyder et al. 1997) and Mir kimberlites (Beard et al. 1996).

From the analyzed mineral pairs of garnet–clinopyroxene, Sm–Nd isochrons yield ages of 1,070 ±5 Ma (initial ϵ_{Nd} = +3.9) for sample O-81/91, and 1,223 ±3 Ma (ϵ_{Nd} = −12.4) for sample O-84/91 (Fig. 9). When the analytical data of orthopyroxene and chlorite in sample O-84/91 are also combined in the isochron calculation, it defines a similar age (1,199 ±225 Ma) but with a higher initial ϵ_{Nd} (−8.5). Similarly, regression through garnet–clinopyroxene Sm–Nd isotopic data for the two samples O-81/91 and O-84/91, including their reconstructed whole-rock isotopic composition, yields ages of 1,071 ±23 and 1,237 ±5 Ma, respectively. All these isochron ages are much older than the Cretaceous age of the Obnazhennaya kimberlite eruption. Samples enriched to the degree of O-84/91 are uncommon but have been recognized in diamond-bearing kimberlite pipes of Mir and Udachnaya (Beard et al. 1996; Snyder et al. 1997). The xenoliths analyzed to date from the Obnazhennaya kimberlite pipe, including the ages determined by McCulloch (1986), yield garnet–clinopyroxene isochron ages which are of mid- to late-Proterozoic ages. These are considerably younger than the

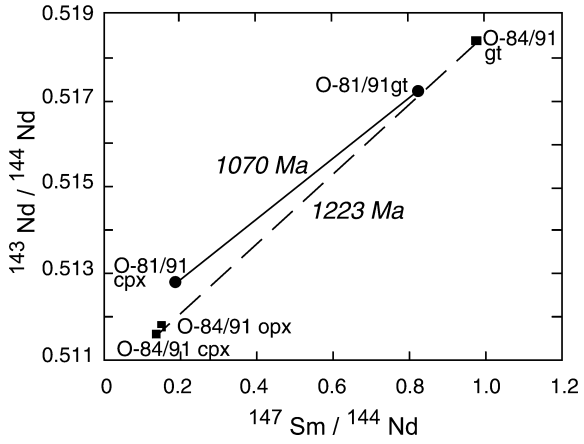

Fig. 9 Plot of $^{143}Nd/^{144}Nd$ versus $^{147}Sm/^{144}Nd$ for two group A websterites from the Obnazhennaya kimberlite pipe, and their mid- to late-Proterozoic isochron ages

Re–Os ages obtained from the eclogite xenoliths in the Udachnaya kimberlite (2.9–3.1 Ga; Pearson et al. 1995).

Discussion

Formation of group B eclogites

The group B eclogite xenoliths (O-501, O-927, O-82/91) from the Obnazhennaya kimberlite pipe show chemical features comparable to group B eclogites from the Udachnaya and Mir kimberlites (Beard et al. 1996; Snyder et al. 1997; Sobolev et al. 1998a, 1998b), as well as group B eclogites worldwide. Major-element compositional features of garnet and clinopyroxene are shown in Figs. 2, 3, and 4. The only difference observed from these Yakutia localities is that the Na_2O contents in garnets from the Obnazhennaya kimberlite are systematically lower than those from the Udachnaya kimberlite. Major-element bulk compositions of these eclogites were estimated from the compositions of the primary constituent minerals and their modes (Table 8). The results are close to that of the mid-ocean ridge basalt (MORB; Hofmann 1988), supporting the origin from subducted oceanic crust. Additionally, $\delta^{18}O$ compositions of these samples (6.32–7.81‰) are well outside the mantle range of 5.5 ± 0.4‰ (Mattey et al. 1994). High oxygen isotopic ratios, like those observed from portions of some ophiolites, are caused by rock interactions with low-T hydrothermal water (Gregory and Taylor 1981). Garnets from these samples show slight to medium positive Eu anomalies, with Eu/Eu* of 1.2–1.5. Positive Eu anomalies in eclogite have been interpreted as a crustal signature resulting from the accumulation of plagioclase in the protolith (MacGregor and Manton 1986; Shervais et al. 1988; Taylor and Neal 1989; Taylor 1993; Aulbach et al. 2002). All these observations are consistent with and support the subduction origin of the group B eclogites.

Table 8 Estimated bulk major-element compositions of eclogite (*E*) and websterite (*W*) xenoliths sorted by groups A and B

Sample	O-82/91	O-501	O-927	O-423	O-926	O-1073	O-1103	O-1108	O-4	O-81/91	O-83/91	O-84/91	O-85/91	O-86/91	O-901	O-1085	O-1101	O-1109	Kaapvaal[a]	Abyssal[a]	Pyrolite[a]	MORB[a]
	E	E	E	E	E	E	E	E	W	W	W	W	W	W	W	W	W	W				
Group	B	B	B	A	A	A	A	A	A	A	A	A	A	A	A	A	A	A				
SiO_2	42.8	46.4	49.7	50.1	50.4	49.6	48.4	49.4	50.0	47.7	47.7	49.4	48.3	49.2	50.0	47.1	48.4	49.3	46.6	43.6	45.0	50.2
Al_2O_3	18.5	16.2	12.3	12.9	11.7	10.8	14.1	12.9	9.03	15.0	14.1	13.0	13.5	13.3	12.8	15.5	10.5	13.6	1.46	1.18	4.45	15.4
TiO_2	0.15	0.22	0.20	0.04	0.11	0.10	0.34	0.47	0.07	0.23	0.22	0.23	0.08	0.29	0.36	0.14	0.09	0.42	0.04	0.02	0.20	1.43
Cr_2O_3	0.06	0.06	0.09	0.21	0.19	0.32	0.11	0.62	0.38	0.32	0.18	0.26	0.23	0.20	0.55	0.04	0.38	0.28	0.40	0.22	0.38	
FeO	13.2	11.2	8.07	3.75	6.53	8.49	6.90	4.67	8.76	7.41	7.02	4.52	8.55	7.29	5.35	9.19	9.61	4.13	6.24	8.22	8.05	10.3
MnO	0.23	0.20	0.14	0.08	0.13	0.18	0.19	0.16	0.22	0.17	0.15	0.14	0.19	0.17	0.14	0.14	0.20	0.13	0.12	0.14	0.14	0.19
MgO	11.3	11.3	13.0	14.8	14.8	15.0	15.3	15.0	15.9	19.7	17.8	19.6	15.4	17.2	14.6	16.4	16.1	17.7	44.1	45.2	37.8	8.07
CaO	10.9	12.1	13.8	15.5	13.7	14.0	12.0	13.7	14.8	8.50	10.9	11.0	11.5	10.2	12.4	9.86	13.4	12.2	0.79	1.13	3.55	11.6
Na_2O	1.27	2.20	2.61	2.10	2.32	1.41	2.21	2.53	0.98	1.02	1.46	1.49	1.75	2.30	3.11	1.29	0.86	2.04	0.09	0.02	0.36	2.62
K_2O	<0.03	<0.03	<0.03	<0.03	<0.03	<0.03	<0.03	<0.03	<0.03	<0.03	<0.03	<0.03	<0.03	<0.03	<0.03	<0.03	<0.03	<0.03				0.10
Total	98.40	99.84	99.98	99.49	99.79	99.87	99.64	99.42	99.91	100.07	99.46	99.56	99.58	99.48	99.37	99.68	99.57	99.79	100.03	99.95	100.00	100.00
Mg/(Mg+Fe)	0.608	0.644	0.744	0.877	0.803	0.761	0.800	0.870	0.765	0.827	0.820	0.886	0.764	0.809	0.831	0.779	0.766	0.885	0.926	0.907	0.893	0.582

[a]Compositions of Kaapvaal and abyssal peridotites are from Boyd (1989), pyrolite from McDonough and Sun (1995), and MORB from Hofmann (1988)

Some apparent differences exist in major-element and REE compositions between MORB and the group B eclogitic xenoliths. The Mg# range of the bulk eclogites is 0.61–0.74. These values are higher than MORB (0.58), indicating a relatively refractory feature of the studied group B eclogites, as compared with MORB, possibly as a result of extraction of a TTG partial melt as part of the subduction process (e.g., Ireland et al. 1994). This is also reflected in lower contents of SiO_2 (42.8–49.7 wt%), TiO_2 (0.15–0.22 wt%), and particularly K_2O (< 0.03 wt%). Contents of these elements in MORB are 50.2, 1.43, and 0.1 wt%, respectively. Estimated bulk REE concentrations of the group B eclogites are shown in Fig. 10, together with those of MORB. The pattern of eclogite O-82/91 is close to MORB; however, samples O-501 and O-927 are richer in LREEs. Particularly, sample O-927 exhibits an enriched pattern in LREEs, with La/Yb of 2.7. It should be pointed out that bulk CaO contents in O-501 and O-927 (12.1 and 13.8 wt%, respectively) are higher than that in MORB (11.6 wt%). It seems that LREE contents of the bulk group B eclogites increase together with their CaO contents. The relatively refractory major-element features and the large variations of REE concentrations demonstrate that these group B eclogites are not simply formed as subsolidus recrystallization of the subducted oceanic crust. Partial melting and secondary enrichment processes have also been involved in the formation of these group B eclogites, during the subduction of oceanic crust, as suggested by several studies (e.g., Ireland et al. 1994; Taylor et al. 1996).

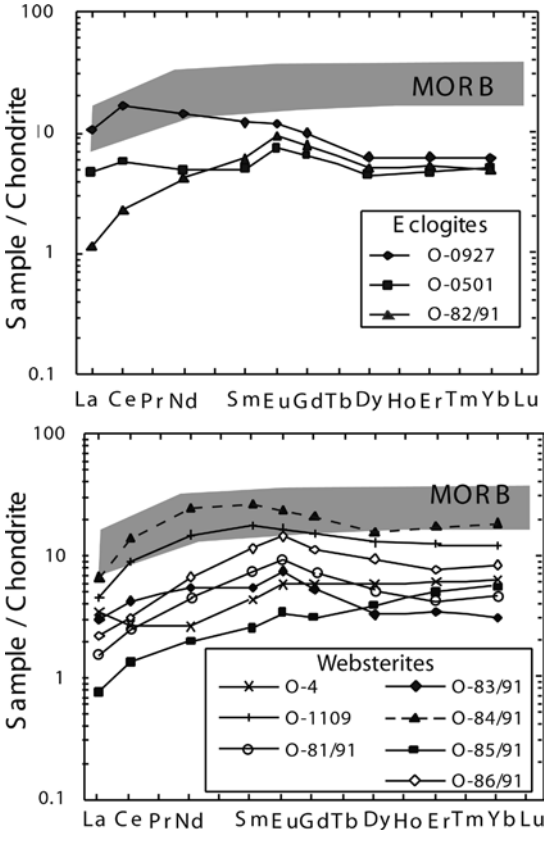

Fig. 10 Reconstructed bulk REE concentrations of eclogite (*above*) and websterite (*below*) xenoliths from the Obnazhennaya kimberlite pipe, estimated from the REE concentrations in minerals and their modes. Range of REE abundances from typical N-MORB is shown by the *shaded area* (BVTP 1981; Schilling et al. 1983)

Formation of group A eclogites

It is generally accepted that the group B and C eclogites originated from subducted oceanic crust. By contrast, the petrogenesis of the group A eclogites has always remained an enigma. Some workers have concluded that these xenoliths originated in the mantle (e.g., Smyth et al. 1989; Taylor and Neal 1989). Others have speculated that these samples may also be of oceanic affinity and are remnants of deeper, ultramafic oceanic crust, akin to the harzburgitic to gabbroic sections of ophiolites which also contain pods of chromite (MacGregor and Manton 1986; Jacob et al. 1994; also see Snyder et al. 1997, for a discussion).

As shown above, compared with mantle peridotites and the group B eclogites, minerals in the group A eclogites/websterites exhibit clear transitional chemical features (Figs. 2, 3, and 4). Bulk major-element compositions of these group A xenoliths are listed in Table 8, estimated in the same way as that for the group B eclogites. These show intermediate amounts of SiO_2 (47.0–50.3 wt%) and significant amounts of Al_2O_3 (9.0–15.5 wt%), FeO (3.8–9.6 wt%), MgO (14.6–19.7 wt%), and CaO (8.5–14.7 wt%). On the other hand, they also contain significant Cr_2O_3 (0.3–0.6 wt%) and Na_2O (1.0–3.1 wt%). As listed in Table 8, these compositional features are entirely different from peridotite, with various degrees of depletion, and MORB. The bulk chemistry of the group A eclogites is also different from komatiite or picrite, by its high CaO and Na_2O contents; indeed, compositions of the group A eclogites are not comparable to any known magmatic rock. Therefore, the group A eclogites are probably not formed directly through crystallization of a melt in the mantle, contrary to what we originally thought (e.g., Shervais et al. 1988; Taylor and Neal 1989; Neal et al. 1990).

Bulk REE concentrations of the group A eclogites are plotted in Fig. 10. A large range in LREE contents are present, with La_n of 0.75 to 6.3, and most of the patterns are nearly flat or only slightly depleted in LREEs. Concentrations of LREEs in most samples are lower than those of MORB or abyssal peridotite. Many of the studied group A eclogites from the Obnazhennaya kimberlite exhibit evidences of crustal origin, as detailed above. Garnets from four group A eclogites and websterites possess positive Eu anomalies (O-423, O-1073, O-81/91, O-83/91), with Eu/Eu* of 1.2–1.4 (Fig. 6), a signature of plagioclase involvement (i.e., low P) at some stage in their genesis. Additionally, the majority of the garnets from the other group A eclogites are above the

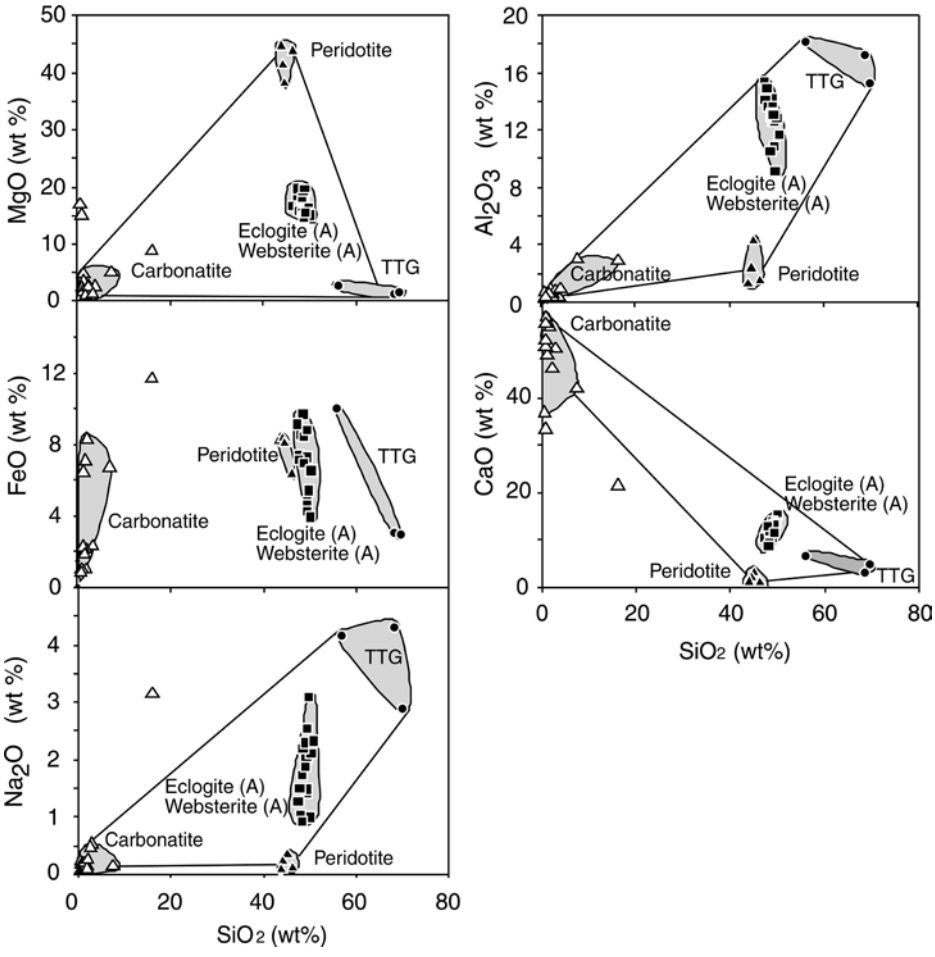

Fig. 11 Summary of major-element variations among mantle peridotite, carbonatite melt, TTG melt (tonalite–trondhjemite–granodiorite), and the bulk composition of the group A eclogite/websterite suite from the Obnazhennaya kimberlite pipe. This indicates that the group A eclogites can be formed through the reaction of TTG and carbonatite melts with mantle peridotite

mantle-oxygen isotopic range. These features preclude a simple mantle origin for the group A eclogites. In addition, the distinct bulk major-element compositions of the group A eclogites described above are not consistent with a model of partial melting and crystallization in the mantle (Shervais et al. 1988).

Partial melting of subducted oceanic crust leads to the formation of the tonalite–trondhjemite–granodiorite (TTG) melts which are rich in SiO_2, Al_2O_3, and Na_2O (e.g., Ireland et al. 1994, Rudnick 1995). Consequently, the resulting ''restites'' are relatively depleted in these components. Such a compositional relation simply rules out the possibility that the group A eclogites are residual parts from partial melting of the subducted oceanic crust. The group A eclogites have the same compositional ranges as MORB, in SiO_2, Al_2O_3 and Na_2O. When partially melted, REEs are strongly partitioned into the melt. Low REE concentrations in the bulk group A eclogites relative to MORB, however, is indicative of a melt-depletion event. Nevertheless, the group A characteristics are crustal, thereby necessitating an additional component to be added to the subducted eclogite crust. In this respect, we postulate that the depleted mantle peridotites may be the source of these group A eclogites and websterites. Interaction of depleted peridotite with upward percolating TTG and carbonatitic melts, derived from the devolatilizing subducted oceanic crust, may have resulted in the formation of group A eclogites and websterites.

For peridotite, high-pressure experiments demonstrated that the compositions of melts change gradually with pressure. Melt produced in the partial melting of a fertile peridotite is basaltic at pressures less than 3.0 GPa, picritic at about 3.0–4.0 GPa, and komatiitic at 5.0–7.0 GPa (Takahashi 1986; Takahashi et al. 1993). As shown in Fig. 5, the equilibrium pressures of the studied group A eclogites/websterites are of 2.0–4.0 GPa. Melt generated in this pressure range would be basaltic-picritic. This would be entirely different from the bulk compositions of these group A eclogites in terms of MgO, FeO, and Cr_2O_3 contents. Therefore, additional chemical components are needed to explain the current observations.

Hybrid crust/mantle reaction model

Partial melting and fluid/rock metasomatism are common in the upper mantle, particularly in subduction-related regions. However, the total significance of these processes in the petrogenesis of mantle rocks is not well understood. Here, we propose a scenario in which the partial melting of subducted oceanic crust and melt/rock reactions are

involved in the formation of the group A eclogites, and associated websterites from Obnazhennaya.

When subduction begins, a series of processes occur with increasing pressure and temperature initiated by devolatilization. At depths corresponding to 20–40 kbar, the temperature of the subducted oceanic crust is sufficiently high such that partial melting occurs. Two types of melts can be produced. One is the SiO_2-, Al_2O_3-, and Na_2O-rich, FeO-, MgO-poor TTG melt (Tatsumi 1982; Tatsumi and Ishizaka 1982; Rapp and Watson 1995; Rapp et al. 1999). Another is a CO_2-rich carbonatite melt, formed by melting of carbonate-rich oceanic sediments. Upon ascending, these melts react with the overlying peridotite mantle wedge. In this scenario, the peridotite is hybridized by both TTG and carbonatite melts/fluids to form group A eclogites.

A combination of interaction of carbonatite and TTG melts with mantle peridotite can reasonably illustrate all the major-element features of the group A eclogites and websterites (Fig. 11). Elevated contents of Cr_2O_3 in garnet and clinopyroxene are common features of group A eclogites. Being a refractory element, Cr_2O_3 is typically concentrated in the depleted peridotite in the mantle wedge. Reaction of such a depleted peridotite with the TTG and carbonatite melts can reasonably explain the high Cr_2O_3 content in group A eclogites and websterites. Additionally, this scenario can reasonably explain the oxygen isotopes. Feldspar fractionation is common within the oceanic crust (e.g., anorthositic gabbros in ophiolites), leading to local positive Eu anomaly. When such protoliths are being involved in the partial melting during subduction of the slab, the partial melts will preserve this Eu geochemical signature. This explains the observed positive Eu anomalies in some of the group A eclogites and websterites.

A schematic representation of the generation and movement of these slab melts, within a tectonic framework, is illustrated in Fig. 12. Despite the relative paucity of carbonatite eruptions to the surface of the Earth, recent investigations of mantle peridotites from worldwide locales have demonstrated that carbonatitic melts have played a much larger role in mantle processes than previously appreciated (Hauri et al. 1993; Rudnick et al. 1993; Yaxley et al. 1998; Coltorti et al. 1999). Such activity may strongly modify the mineralogical and geochemical features of the mantle rocks. The sources of the carbonatite melt in our model are uncertain. Some may be of true mantle origin, whereas a portion may be genetically related to the oceanic carbonate sediments. The Sm–Nd isochron ages, as shown in Fig. 9, would appear to indicate that such processes were active in mid- to late-Proterozoic times, possibly indicating that subduction was active beneath the Siberia platform to this late time.

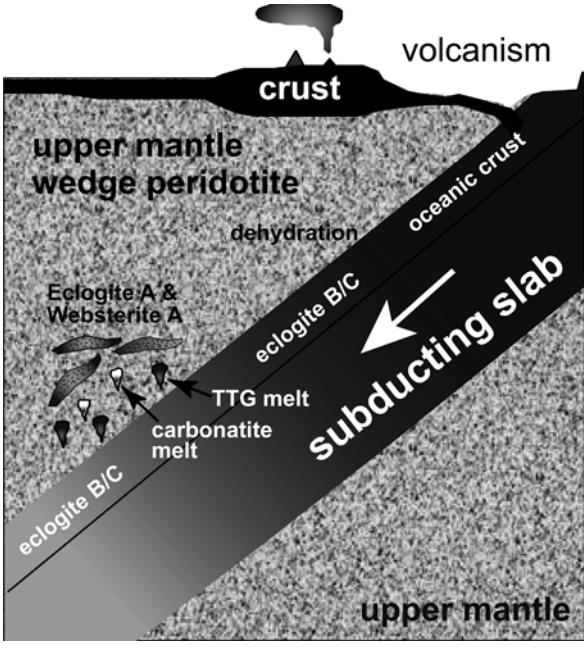

Fig. 12 A model for the formation of group A eclogite/websterite suite in the mantle. The TTG melts are generated by the partial melting of subducted oceanic crust. The carbonatite melt may be of mantle origin but may also be related to the oceanic carbonate sediments. Hybrid reactions of these melts with mantle peridotite, with different degrees of depletion, lead to the formation of the group A suite, some of which were brought to the surface of the Earth by kimberlitic magmatism

Summary

The Obnazhennaya kimberlite pipe in Yakutia is a unusual occurrence of predominantly group A eclogite and websterite xenoliths. Investigation of these samples in the present study has led to several significant conclusions.

- In major-element chemistry, the group A eclogites and websterites exhibit transitional features between the group B eclogites and peridotite.
- Differences in LREEs exist between the Obnazhennaya group A and group B eclogites from Udachnaya. Group A garnets are relatively poorer in LREEs than those from the group B eclogites; however, clinopyroxenes show contrary LREE trends.
- Several significant signatures for crustal components exist in the group A eclogites and websterites, including high $\delta^{18}O$ values and + Eu anomalies.
- It is estimated that these group A eclogites/websterites and peridotites formed at 21–38 kbar and 710–925 °C, between 1,071 and 1,237 Ma ago.
- A scenario for the formation of group A eclogites/websterites involves the reaction of depleted mantle peridotite with TTG and carbonatite melts, during subduction. This scheme may be applicable worldwide.

Acknowledgments We would like to thank Allan Patchen for his assistance with the electron microprobe analyses at the University

of Tennessee, Nobu Shimizu for his assistance with the SIMS analyses, and Masa Kurosawa, University of Tsukuba for assistance with the LA-ICP-MS analyses. Vladimir Sobolev, Alfredo Camacho, and Prinya Promprated are thanked for their stimulating, provocative comments and assistance. Constructive and insightful comments from anonymous reviewers substantially helped to improve the quality of the manuscript. The handling of this manuscript by Dr. Tim Grove is greatly acknowledged. A major portion of this research was supported by NSF grants EAR 97-25885 and EAR 99-09430, for which we are grateful.

References

Aulbach S, Stachel T, Viljoen KS, Brey GP, Harris JW (2002) Eclogitic and websteritic diamond sources beneath the Limpopo Belt—is slab-melting the link? Contrib Mineral Petrol 143:56–70

Beard BL, Fraracci KN, Taylor LA, Snyder GA, Clayton RN, Mayeda TK, Sobolev NV (1996) Petrography and geochemistry of eclogites from the Mir kimberlite, Yakutia, Russia. Contrib Mineral Petrol 125:293–310

Boyd FR (1989) Compositional distinction between oceanic and cratonic lithosphere. Earth Planet Sci Lett 96:15–26

Boyd FR, Pearson DG, Nixon PH, Mertzman SA (1993) Low-calcium garnet herzburgites from South Africa: their relations to craton structure and diamond crystallization. Contrib Mineral Petrol 113:352–366

Boyd FR, Pokhilenko NP, Pearson DG, Mertzman SA, Sobolev NV, Finger LW (1997) Composition of the Siberian cratonic mantle: evidence from Udachnaya peridotite xenoliths. Contrib Mineral Petrol 128:228–246

Brey GP, Köhler T (1990) Geothermobarometry in four-phase lherzolites II: new thermobarometers, and practical assessment of existing thermobarometers. J Petrol 31:1353–1378

BVTP (1981) Basaltic volcanism on the terrestrial planets (Lunar and Planetary Institute). Pergamon Press, New York

Cocker JD, Griffin BJ, Muehlenbachs K (1982) Oxygen and carbon isotope evidence for seawater-hydrothermal alteration of the Macquarie Island ophiolite. Earth Planet Sci Lett 61:112–122

Coleman RG, Lee ED, Beatty LB, Brannock WW (1965) Eclogites and eclogites: their differences and similarities. Geol Soc Am Bull 76:483–508

Coltorti M, Bonadiman C, Hinton RW, Siena F, Upton BGJ (1999) Carbonatite metasomatism of the oceanic upper mantle: evidence from clinopyroxenes and glasses in ultramafic xenoliths of Grande Comore, Indian Ocean. J Petrol 40:133–165

Crowe DE, Valley JW, Baker KL (1990) Microanalysis of sulfur-isotope ratios and zonation by laser microprobe. Geochim Cosmochim Acta 54:2075–2092

Davis GL, Sobolev NV, Khar'kiv AD (1980) New data on the age of Yakutian kimberlites obtained by uranium-lead method on zircons. Dokl Akad Nauk SSSR 254:175–179

DePaolo DJ, Wasserburg GJ (1976) Nd isotopic variations and petrogenetic models. Geophys Res Lett 3:249–252

Elsenheimer D, Valley JW (1992) In situ oxygen isotope analysis of feldspar and quartz by Nd-YAG laser microprobe. Chem Geol 101:21–42

Elsenheimer D, Valley JW (1993) Submillimeter scale zonation of delta-O-18 in quartz and feldspar, Isle-of-skye, Scotland. Geochim Cosmochim Acta 57:3669–3676

Finnerty AA, Boyd FR (1984) Evaluation of geothermobarometers for garnet peridotites. Geochim Cosmochim Acta 48:15–27

Fung AT, Haggerty SE (1995) Petrography and mineral compositions of eclogites from the Koidu kimberlite complex, Sierra-Leone. J Geophys Res 100:20451–20473

Gregory RT, Taylor HP (1981) An oxygen isotope profile in a section of Cretaceous oceanic crust, Samail ophiolite, Oman: evidence for δ^{18}O-buffering of the oceans by deep (>5 km) seawater-hydrothermal circulation at mid-ocean ridges. J Geophys Res 86:2737–2755

Griffin WL, Kaminsky FV, Ryan CG, O'Reilly SY, Win TT, Ilupin IP (1996) Thermal state and composition of the lithospheric mantle beneath the Daldyn kimberlite field, Yakutia. Tectonophysics 262:19–33

Harris JW, Duncan DJ, Zhang F, Miao Q, Zhu Y (1994) The physical characteristics and syngenetic inclusion geochemistry of diamonds from Pipe 50, Liaoning Province, People's Republic of China. In: Meyer HOA, Leonardos OH (eds) Proc 5th Int Kimberlite Conf, vol 2. Diamonds: characterization, genesis and exploration. Brasilia, CPRM Spec Publ 1/B, pp 106–115

Hauri EH, Shimizu N, Dieu JJ, Hart SR (1993) Evidence for hotspot-related carbonatite metasomatism in the oceanic upper mantle. Nature 365:221–227

Helmstaedt H, Doig R (1975) Eclogite nodules from kimberlite pipes of the Colorado plateau—samples of Fransican-type oceanic lithosphere. Phys Chem Earth 9:95–111

Hofmann AW (1988) Chemical differentiation of the earth: the relationship between mantle, continental crust, and oceanic crust. Earth Planet Sci Lett 90:297–314

Hunter RH, Taylor LA (1982) Instability of garnet from the mantle—glass as evidence of metasomatic melting. Geology 10:617–620

Ireland TR, Rudnick RL, Spetsius ZV (1994) Trace elements in diamond inclusions from eclogites reveal a link to Archean granites. Earth Planet Sci Lett 128:199–213

Jacob D, Jagoutz E, Lowry D, Mattey D, Kudrjavtseva G (1994) Trace elements in diamondiferous eclogites from Siberia: remnants of Archean oceanic crust. Geochim Cosmochim Acta 58:5191–5207

Jerde EA, Taylor LA, Crozaz G, Sobolev NV, Sobolev VN (1993) Diamondiferous eclogites from Yakutia, Siberia: evidence for a diversity of protoliths. Contrib Mineral Petrol 114:189–202

Johnson KTM, Dick HJB, Shimizu N (1990) Melting in the oceanic upper mantle: ion microprobe study of diopsides in abyssal peridotites. J Geophys Res 95:2661–2678

Lee D-C, Halliday AN, Hunter RH, Holden P, Upton BGJ (1993) Rb-Sr and Sm-Nd isotopic variations in dissected crustal xenoliths. Geochim Cosmochim Acta 57:219–230

MacGregor ID, Manton WI (1986) Roberts Victor eclogites: ancient oceanic crust. J Geophys Res 91:14063–14079

Mattey D, Lowry D, MacPherson C (1994) Oxygen isotope composition of mantle peridotite. Earth Planet Sci Lett 128:231–241

McCulloch MT (1989) Sm-Nd systematics in eclogite and garnet peridotite nodules from kimberlites: implications for the early differentiation of the earth. In: Ross J et al. (eds) Kimberlites and related rocks, vol 2. Geological Society of Australia, Perth, pp 864–876

McDonough WF, Sun S (1995) The composition of the earth. Chem Geol 120:223–253

Mercier JCC (1976) Single-pyroxene geothermometry and geobarometry. Am Mineral 61:603–615

Mercier JCC (1980) Single-pyroxene thermobarometry. Tectonophysics 70:1–37

Milashev VA, Shul'gina NI (1959) New data on the age of the kimberlites of the Siberian Platform. Dokl Akad Nauk SSSR 126:1320–1322

Neal CR, Taylor LA, Davidson JP, Holden P, Halliday AN, Nixon PH, Paces JB, Clayton RN, Mayeda TK (1990) Eclogites with oceanic crustal and mantle signatures from the Bellsbank kimberlite, South Africa, part 2. Sr, Nd, and O isotope geochemistry. Earth Planet Sci Lett 99:362–379

Nimis P, Taylor WR (2000) Single clinopyroxene geothermobarometer for garnet peridotites. Part I. Calibration and testing of a Cr-in-Cpx barometer and an enstatite-in-Cpx thermometer. Contrib Mineral Petrol 139:541–554

Ouchinnikov YI (1989) Comparative characteristics of deep-seated inclusions from the Obnazhennaya kimberlite pipe (Yakutia) and alkaline basalts of Khakassia. PhD Thesis, Inst Geol Geophys, Novosibirsk

Pearson DG, Boyd FR, Haggerty SE, Pasteris JD, Field SW, Nixon PH, Pokhilenko NP (1994) Characterization and origin of graphite in cratonic lithospheric mantle: a petrological carbon isotope and Raman spectroscopic study. Contrib Mineral Petrol 115:449–466

Pearson DG, Snyder GA, Shirey SB, Taylor LA, Carlson RW, Sobolev NV (1995) Archean Re-Os age for Siberian eclogites and constraints on Archean tectonics. Nature 374:711–713

Qi Q, Taylor LA, Snyder GA, Sobolev NV (1994) Eclogites from the Obnazhennaya kimberlite pipe, Yakutia, Russia. Int Geol Rev 36:911–924

Qi Q, Taylor LA, Snyder GA, Clayton RN, Mayeda TK, Sobolev NV (1997) Detailed petrology and geochemistry of a rare corundum eclogite xenolith from Obnazhennaya, Yakutia. In: Sobolev NV, Mitchell RH (eds) Proc 6th Int Kimberlite Conf, August 1995, Novosibirsk. Allerton Press, New York, pp 247–260

Rapp RP, Watson EB (1995) Dehydration melting of metabasalt at 8-32-kbar—implications for continental growth and crust-mantle recycling. J Petrol 36:891–931

Rapp RP, Shimizu N, Norman MD, Applegate GS (1999) Reaction between slab-derived melts and peridotite in the mantle wedge: experimental constraints at 3.8 GPa. Chem Geol 160:335–356

Rosen OM, Condie KC, Natapov LM, Nozhkin AD (1994) Archean and early Proterozoic evolution of the Siberian craton: a preliminary assessment. In: Condie KC (ed) Archean crustal evolution. Elsevier, Amsterdam, pp 411–459

Rudnick RL (1995) Making continental crust. Nature 378:571–578

Rudnick RL, McDonough WF, Chappell BW (1993) Carbonatite metasomatism in the northern Tanzanian mantle: petrography and geochemical characteristics. Earth Planet Sci Lett 114:463–475

Schilling JG, Zajac M, Evans R, Johnson T, White W, Devine JD, Kingsley R (1983) Petrologic and geochemical variations along the Mid-Atlantic Ridge from 29°N to 73°N. Am J Sci 283:510–586

Shervais JW, Taylor LA, Lugmair GW, Clayton RN, Mayeda TK, Korotev RL (1988) Early Proterozoic oceanic crust and the evolution of subcontinental mantle: Eclogites and related rocks from southern Africa. Geol Soc Am Bull 100:411–423

Shimizu N, Hart SR (1982) Applications of the ion probe to geochemistry and cosmochemistry. Annu Rev Earth Planet Sci 10:483–526

Shimizu N, Semet MP, Allegre CJ (1978) Geochemical applications of quantitative ion microprobe analysis. Geochim Cosmochim Acta 42:1321–1334

Smyth JR, Caporuscio FA, Mccormick TC (1989) Mantle eclogites—evidences of igneous fractionation in the mantle. Earth Planet Sci Lett 93:133–141

Snyder GA, Lee DC, Taylor LA, Halliday AN, Jerde EA (1994) Evolution of the upper mantle of the Earth's moon: Sm and Sr isotopic constraints from high-Ti mare basalts. Geochim Cosmochim Acta 58:4795–4808

Snyder GA, Taylor LA, Jerde EA, Clayton RN, Mayeda TK, Deines P, Rossman GR, Sobolev NV (1995) Archean mantle heterogeneity and the origin of diamondiferous eclogites, Siberia: evidence from stable isotopes and hydroxyl in garnet. Am Mineral 80:799–809

Snyder GA, Taylor LA, Crozaz G, Halliday AN, Beard BL, Sobolev VN, Sobolev NV (1997) The origins of Yakutian eclogite xenoliths. J Petrol 38:85–113

Snyder GA, Keller RA, Taylor LA, Remley DA, Sobolev NV (1998) The origin of ultramafic (Group A) eclogites: Nd and Sr isotopic evidence from the Obnazhennaya kimberlite, Yakutia. In: Ext Abstr Vol 7th Int Kimberlite Conf, April 1998, Cape Town, pp 423–426

Sobolev NV (1977) Deep-seated inclusions in kimberlites and the problem of the composition of the upper-mantle. American Geophysical Union, Washington, DC

Sobolev NV, Lavrent'yev YG (1971) Isomorphic sodium admixture in garnets formed at high pressures. Contrib Mineral Petrol 31:1–12

Sobolev VN, Taylor LA, Snyder GA, Sobolev NV (1994) Diamondiferous eclogites from the Udachnaya kimberlite pipe, Yakutia. Int Geol Rev 36:42–64

Sobolev NV, Snyder GA, Taylor LA, Keller RA, Yefimova ES, Sobolev VN, Shimizu (1998a) Extreme chemical diversity in the mantle during eclogitic diamond formation: Evidence from 35 garnet and 5 pyroxene inclusions in a single diamond. Int Geol Rev 40:567–578

Sobolev NV, Taylor LA, Zuev VM, Bezborodov SM, Snyder GA, Sobolev VN, Yefimova ES (1998b) The specific features of eclogitic paragenesis of diamonds from Mir and Udachnaya kimberlite pipes (Yakutia). Russian Geol Geophys 39:1653–1663

Sobolev VN, McCammon CA, Taylor LA, Snyder GA, Sobolev NV (1999) Precise Mössbauer milliprobe determination of ferric iron in rock-forming minerals and limitations of electron microprobe. Am Mineral 84:78–85

Spetsius ZV, Serenko VP (1990) Composition of continental upper mantle and lower crust under the Siberian platform. Results of Researches on the International Geophysical Projects, pp 272

Spetsius ZV, Taylor LA (2002) Partial melting in mantle eclogite xenoliths: clues to microdiamond genesis. Int Geol Rev 44:973–987

Stachel T, Harris JW (1997a) Diamond precipitation and mantle metasomatism—evidence from the trace element chemistry of silicate inclusions in diamonds from Akwatia, Ghana. Contrib Mineral Petrol 129:143–154

Stachel T, Harris JW (1997b) Syngenetic inclusions in diamonds from the Birim field (Ghana)—a deep peridotitic profile with a history of depletion and re-enrichment. Contrib Mineral Petrol 127:336–352

Takahashi E (1986) Melting of a dry peridotite KLB-1 up to 14 GPa: implications on the origin of peridotite upper mantle. J Geophys Res 91:9367–9382

Takahashi E, Shimazaki T, Tsuzaki Y, Yoshido H (1993) Melting study of peridotite KLB-1 to 6.5 GPa and the origin of basaltic magmas. Philos Trans R Soc Lond A 342:105–120

Tatsumi Y (1982) Origin of high-magnesian andesites in the Setouchi volcanic belt, southwest Japan. 2. Melting phase-relations at high-pressures. Earth Planet Sci Lett 60:305–317

Tatsumi Y, Ishizaka K (1982) Origin of high-Magsesian andesites in the Setouchi volcanic belt, southwest Japan. 1. Petrographic and chemical characterics. Earth Planet Sci Lett 60:293–304

Taylor LA (1993) Evolution of the subcontinental mantle beneath the Kaapvaal craton: a review of evidence for crustal subduction for Bellsbank eclogites. In: VS Sobolev Memorial Volume, Geol Geofiz 34:25–47

Taylor LA, Neal CR (1989) Eclogites with oceanic crustal and mantle signatures from the Bellsbank kimberlite, South Africa, Part I. Mineralogy, petrography, and whole rock chemistry. J Geol 97:551–567

Taylor LA, Snyder GA, Crozaz G, Sobolev VN, Yefimova ES, Sobolev NV (1996) Eclogitic inclusions in diamonds: evidence of complex mantle processes over time. Earth Planet Sci Lett 142:535–551

Taylor LA, Milledge HJ, Bulanova G, Snyder GA, Keller RA (1998) Metasomatic eclogitic diamond growth: evidence from multiple diamond inclusions. Int Geol Rev 40:595–612

Taylor LA, Keller RA, Snyder GA, Wang W, Carlson WD, Hauri EH, McCandless T, Kim K-R, Sobolev NV, Bezborodov SM (2000) Diamonds and their mineral inclusions and what they tell us: a detailed "pull-apart" of a diamondiferous eclogite. Int Geol Rev 42(12):959–983

Ukhanov AV, Khar'kiv AD, Ryabchikov ID (1988) Lithospheric mantle of Yakutian kimberlite province (in Russian). Nauka, Moscow

Ustinov VI, Ukhanov AV, Grinenko VA (1981) Oxygen-isotope compositions of mantle xenoliths from the Obnazhennaya kimberlite pipe in north Yakutia. Geokhimiya 6:937–941

Ustinov VI, Ukhanov AV, Grinenko VA, Gavrilov YY (1987) $\delta^{18}O$ in eclogites from the Udachnaya and Obnazhennaya kimberlite pipes. Geokhimiya 11:1637–1641

Viljoen KS, Smith CB, Sharp ZD (1996) Stable and radiogenic isotope study of eclogite xenoliths from the Orapa kimberlite, Botswana. Chem Geol 131:235–255

Xu XS, O'Reilly SY, Griffin WL, Zhou XM (2000) Genesis of young lithospheric mantle in southeastern China: an LAM-ICPMS trace element study. J Petrol 41:111–148

Yaxley GM, Green DH, Kamenetsky V (1998) Carbonatite metasomatism in the southern Australian lithosphere. J Petrol 39:1917–1930

Zindler A, Jagoutz E (1988) Mantle cryptology. Geochim Cosmochim Acta 52:319–333

Zonenshain LP, Kuzmin MI, Natapov LM (1990) Geology of the USSR: a plate-tectonic synthesis. American Geophysical Union, Washington, DC, Geodynamics Series vol 21